FXNH

AIR FORCE FLIGHT DYNAMICS LABORATORY
DIRECTOR OF LABORATORIES
AIR FORCE SYSTEMS COMMAND
WRIGHT PATTERSON AIR FORCE BASE OHIO

LOW MACH NUMBER TEMPERATURE MEASUREMENTS
USING ENCAPSULATED LIQUID CRYSTALS

Max E. Hillsamer

August 1973

Project Nr. 1366

Approved for public release; distribution unlimited

20000509 149

High Speed Aero Performance Branch
Flight Mechanics Division
Air Force Flight Dynamics Laboratory

LOW MACH NUMBER TEMPERATURE MEASUREMENTS
USING ENCAPSULATED LIQUID CRYSTALS

Max E. Hillsamer

August 1973

Project Nr. 1366

High Speed Aero Performance Branch
Flight Mechanics Division
Air Force Flight Dynamics Laboratory

FOREWORD

This report was prepared by M.E. Hillsamer of the High Speed Aero Performance Branch, Air Force Flight Dynamics Laboratory, Wright-Patterson Air Force Base, Ohio. The work was performed as part of the AFFDL in-house research under Task Nr. 136603 "Aerodynamic Heating to Military Vehicles", Project Nr. 1366 "Aeroperformance and Aeroheating Technology", and covers work conducted between December 1972 and March 1973.

Models for the tests were designed and fabricated under the direction of Mr. John E. Fehl, Aerospace Vehicle Branch (FXS), and tests were conducted by personnel from Aeromechanics Branch (FXM) and Experimental Engineering Branch (FXN) of the Air Force Flight Dynamics Laboratory. The author gratefully acknowledges their cooperative assistance.

This report has been reviewed and is approved.

PHILIP P. ANTONATOS
Chief, Flight Mechanics Division
Air Force Flight Dynamics Laboratory

ii

ABSTRACT

An experimental program was conducted to evaluate the use of encapsulated liquid crystals as a means of determining temperature profiles in regions of interfering flows on wind tunnel models at supersonic speeds. The tests were conducted on both plane surfaces and on an ogive cylinder model equipped with 3 dimensional shock generators at Mach numbers of 1.89 and 3.00 in the Trisonic Gasdynamic Facility of the Air Force Flight Dynamics Laboratory. Freestream Reynolds number were 1.0 and 3.0 million per foot.

Results show that models coated with encapsulated liquid slurry and overcoated with a protective plastic film provided better temperature profiles than models equipped with paper substrated liquid crystals. Temperature profiles were easily discernible over the entire surface of the ogive cylinder model within viewing range of the camera, and specular reflections on the non-planar surfaces did not invalidate any data.

CONTENTS

LIST OF TABLES

ILLUSTRATIONS

LIST OF SYMBOLS

Symbol	Description
M	Mach number, dimensionless
R_e	Reynolds number, 1/ft
r	Recovery factor
T	Temperature, deg F or deg R
X	Axial distance measured from model leading edge, in.
α	Angle of attack, deg.
δ	Fin or canard deflection angle, deg.
γ	Ratio of specific heats
λ	Wavelength of light, nm.

Subscripts

AW	Adiabatic Wall Conditions
F	Fin or canard
0	Total or stagnation conditions
W	Model wall conditions
∞	Freestream conditions

I. INTRODUCTION

Aerodynamic heating of aircraft and missile configurations in the supersonic flight regime, while not so severe as to cause catastrophic failure, can result in degradation of the structure. Of special interest are regions around wing-body or fin-body junctions where localized "hot spots" develop because of intersecting flow fields.

The purpose of the present study was to investigate and evaluate methods of obtaining model surface temperatures and heat transfer rates in regions of interfering flow fields at low Mach numbers.

Several methods have been used in wind tunnels to measure temperatures and heating rates in regions of interfering flow fields at Mach numbers of 6 and above. Neumann and Burke (Reference 1) compare results obtained by them and others in interfering flow fields of 2 and 3-dimensional shock generator models. Models used were thin skin flat plates equipped with standard thermocouple instrumentation. Incomplete mapping of high heating regions resulted because of lack of adequate instrumentation in areas of interest. Thin skin thermocouple instrumented models are also quite costly to build.

Various investigators such as Jones and Hunt (Reference 2) and Patterson (Reference 3) have used a method of obtaining quantitative heat transfer measurements with temperature sensitive phase change coatings applied to models made of low conductivity materials, such as Teflon or Stycast. Schultz (Reference 4) used this phase change

coating method to quantitatively obtain heat transfer rates in inter-
ferfering flow regions on a flat plate model in the AFFDL High Temperature
Facility at Mach 10.

An obvious disadvantage in the use of the phase change coating
technique is that the phase change is not reversible. Model surfaces
must be cleaned and coated before each test run. Also, the Stycast
castable model material used for the model fabrication is not completely
homogeneous, and thermal properties of the material vary from batch
to batch.

McElderry (References 5 and 6) conducted boundary layer transition
studies at supersonic speeds using cholesteric liquid crystals attached
to plexiglass models. The start of transition was determined by the
color change of the liquid crystals due to increases in model surface
temperatures. Klein (References 7 and 8) was probably the first
investigator to report on the use of liquid crystals for aerodynamic
testing.

While the investigations of McElderry and Klein were mainly concerned
with locating boundary layer transition and turbulent regions, the liquid
crystals technique appeared applicable to complete thermal mapping of
models, with special emphasis on regions of interfering flow fields.
Advantages of this method are that model fabrication costs can be low,
complete temperature profiles can be obtained, color changes of the
liquid crystals are reversible, and the liquid crystals are obtainable
over a wide range of lower temperatures suitable for supersonic wind
tunnel facilities.

The present studies evaluated methods of attaching liquid crystals to

2

the models, placement of light sources and cameras, mechanical stresses on the coatings and thermal mapping of the models. No means was available for obtaining temperature-time variations on the models, so transient heat transfer values were not obtained.

II. APPARATUS

a. Models

Four plexiglass models were constructed for use in this study. Plexiglass was chosen for its low thermal conductivity, uniformity of material, and ease of machining.

Two models, identical in size and shape, were used to evaluate methods of attaching liquid crystals. The models were flat plates 8 in. wide, 16 in. long and 3/4 in. thick with sharp leading edges of 15 deg bevel. The top surface of the first model was recessed approximately 0.014 in. from 0.250 in. back of the leading edge to the rear of the model. This recess was provided for mounting plastic covered, paper backed sheets of liquid crystals with two-sided masking tape. A smooth model surface was thereby achieved. The top surface of the second model was not recessed and was painted flat black to provide a dark base for the liquid crystals slurry an alternative to the paper backed sheets previously used.

The third model tested was a flat plate identical to the second model except that the width was 14 in. Use of the wider model assured that flow disturbances from the front corners of the model would not affect the flow in the region of shock generation.

Two shock generators were used with the flat plate models. Each generator was 7 3/4 in. long, 2 in. high and 1 3/8 in. wide with sharp leading edges of 20 deg bevel. The leading edge sweep angle of the first

3

was 0 deg and 30 deg on the second. Holes drilled through the flat plates permitted the shock generators to be bolted on at any desired position. The shock generators were aluminum painted flat black to reduce glare from camera lights.

To evaluate the use of liquid crystals on non-planar surfaces, an ogive cylinder model, 12 in. long and 3 1/4 in. base diameter was fabricated from plexiglass and painted flat black. Two different size canards were supplied for shock generation on the body of the model. Both canards had a leading edge radius of 0.016 in. and a leading edge sweep angle of 57 deg with a trailing edge sweep angle of 10 deg. The larger canard (A) had a base chord of 3.73 in. and a span of 2.62 in., and the smaller canard (B) had a base chord of 1.90 in. and a span of 1.36 in. The canards were equipped with roll pins which were inserted into a hole in the side of the model 2.57 in. forward of the base and held in place with a set screw. Canard angle with respect to the model could thereby be adjusted.

Figure 1 is a sketch of the flat plate models with shock generators. Figure 2 presents the ogive cylinder model with control canards attached.

B. Liquid Crystal Coatings

Cholesteric liquid crystals are chemically cholesterol esters mostly of fatty acids. These nonflammable substances are liquid in mobility but crystalline in optical properties. When illuminated with unpolarized white light, incident at a given angle, only one light wavelength is reflected at each viewing angle. Small temperature changes

cause a shift in the molecular structure of the liquid crystals, and light of a different wavelength is then reflected. Fergason (Reference 9) presents more complete documentation on the properties and characteristics of the liquid crystals.

By selectively mixing liquid crystal substances color changes through the entire visible spectrum can be obtained with increase in temperature. The temperature span of color changes can be as small as 1.8°F or as large as 90°F. Temperatures can be measured with better than 0.18°F accuracy, and reaction time of the liquid crystals to temperature change is less than 0.2 sec. Temperatures at which known liquid crystals operate range from -4°F to 480°F. The color changes of the liquid crystals are reversible, and the substances can be cycled through their temperature ranges any number of times.

Liquid crystals in their raw form are responsive to mechanical stress, electromagnetic radiation and chemical vapors in addition to temperature. The National Cash Register Company (NCR) has an encapsulation process whereby microscopic amounts of liquid crystal compounds are encased in hard spherical shells 10 to 30 microns in diameter. The encapsulated liquid crystals are more stable and less responsive to mechanical stress or chemical vapors.

Encapsulated liquid crystals are available from NCR in either sheet or slurry form. The sheets are made by sandwiching a thin layer of encapsulated liquid crystals between a top sheet of clear plastic and a back of black paper. The sheets are fastened to the model surface with two-sided masking tape. This method was used on the first model tested in the present study.

5

Encapsulated liquid crystals in the slurry form were sprayed
on the surface of the model with an artist's air brush. After the
slurry dried a protective coating of Krylon plastic was applied to
the model surface. A hard, smooth model surface was obtained with a
total coating thickness, including flat black paint, liquid crystals
and Krylon coating, of 1.1 mil. This method of application was used
on one 8 in. wide flat plate and 14 in. wide flat plate and the
ogive cylinder model. All models were coated with NCR type W-15 encapsu-
lated liquid crystals, which has a temperature span of 10.8 deg F from
start of red to start of blue color change. Figure 3 shows the range
and color change temperatures of this particular compound.

C. Wind Tunnel

In-house testing was conducted in the AFFDL Two-Foot Trisonic
Gasdynamics Facility (TGF). This facility is a closed circuit, variable
density, continuous flow wind tunnel using air as the working fluid.
A variation in Mach number from subsonic to Mach 3.0 is provided through
the use of fixed two-dimensional planar nozzle blocks.

Stagnation pressure and temperature can be set by the operator and
are automatically controlled to within ±1 psf and ±1°F respectively.

Figure 4 is a sketch of the general layout of the wind tunnel.
Reference 10 describes the facility and associated equipment in full
detail.

D. Instrumentation

Color photographs of the model at each attitude constituted the
entire model data acquisition. A 4 x 5 graphic view camera was placed
directly normal to the model surface approximately 6 feet from the

6

subject. The light sources were two 500 watt, 3200 kelvin lamps about 30 degrees on each side of, and slightly higher than the camera. Four second exposures at F22 were made on type L Ektacolor film.

III. TEST DESCRIPTION

A. Test Conditions

Tests to compare paper mounted encapsulated liquid crystals (ELC) with slurry coated models were conducted at Mach 1.89 and a freestream Reynolds number about 3 million per foot. Stagnation pressure was 1600 psfa, and stagnation temperature was varied from 100 to 115°F in 5° increments. The two 8 inch wide by 16 inch long flat plates were used during this phase of the test.

The 14 in. wide by 16 in. long flat plate and the ogive cylinder were tested at Mach numbers of 1.89 and 3.00 and freestream Reynolds numbers about one and three million per foot. Table I lists test conditions for each model.

B. Test Procedure

All models were provided with ELC coatings several days before start of the tests and stored so that testing would not be delayed by model preparation. No deterioration in coatings was evident because of storage.

Prior to starting the wind tunnel for each test run, each flat plate model was rolled so the coated surface was in the horizontal plane. After starting the tunnel, the model was rolled 90 deg with the coated surface toward the camera. This starting procedure reduced the danger of the model damaging the windows in case high starting loads would cause

7

the model to break loose.

First test point pictures were taken at the maximum required stagnation pressure and minimum stagnation temperature. The temperature was then increased with photographs obtained every 5 deg. Stagnation pressure and temperature were then reduced to minimum required conditions and the procedure was repeated.

Shock generator fins were tested at the most rearward locations first so that the shock generators would cover the mounting holes in the surface of the model on succeeding runs. During Mach 3 testing the mounting holes toward the front of the flat plate were filled with modelling clay to assure a smooth surface ahead of the shock generator.

The ogive cylinder model, D, was installed with the fin mounting hole toward the camera. Initial test point for each run were at maximum stagnation pressure and minimum stagnation temperature. The model was pitched from 0 deg to 12 deg with test photos being obtained every 4 deg. Stagnation temperature was then increased and the angle-of-attack sequence was repeated.

Table II is a summary of model configurations used during testing in the 2 Ft TGF.

C. Data Reduction

There was no method available for removing the model from the tunnel airflow and providing a time base to obtain transient heat transfer rates. Therefore, all data presented in this report are in the form of temperature distance lines or isothermal line patterns in the region of the shock

8

generators. These isothermal lines were obtained from 8 x 10 in. color
prints of the test photographs taken at each test point.

The standard 2 Ft TGF data reduction was used to provide stagnation
and freestream operating conditions in the wind tunnel.

IV. RESULTS

A. General

Data presented in this report are from two separate test periods in
the 2 Ft TGF. The majority of test time was concentrated in the Mach
1.89 studies, with only sufficient runs at Mach 3.00 to determine the
suitability of the method. Results presented in this report are at a
stagnation temperature of 100°F for Mach 1.89 and 115°F at Mach 3.00.
The higher temperature was necessary to produce color change profiles
at Mach 3.0.

A total of 392 color photographs of model temperature profiles were
obtained during this test. Because of the time involved in reducing
data from all the photographs, only representative temperature profiles
are presented. Reproduction of color photographs is quite costly, so
only representative color prints are presented in this report. Sufficient
fine detail was not obtainable from black-and-white prints of the color
negatives. Temperature profiles presented were obtained by plotting distances
measured from color photographs. None of the data were reduced to heat
transfer coefficients because no adequate time base was available to
determine heating rates.

B. Mach 1.89 Data

The first phase of this study consisted of determining the most suitable method of attaching liquid crystals to the flat plate models. Comparisons of the paper and slurry type mounting methods are presented in figure 5 (a-h). For identical fin locations, high temperature areas are the same on both models. However, much clearer detail is evident on the slurry coated model because of the smoother test surface. The paper backed ELC appeared to bubble and wrinkle when exposed to the tunnel airflow causing tripping of the model boundary layer. Streaks of color on the paper coated model are evidences of this boundary layer tripping. With the fin at its most forward location (fig. 5 g) the entire rear section of paper mounted ELC came off during testing.

Klein (Reference 7) utilized raw (not encapsulated) liquid crystals in the slurry state which were free-flowing during wind tunnel operation. The coating tended to leave regions of high shear, and necessitated recoating the model after a period of testing. His recommendation was to cover the liquid crystals with a thin transparent plastic coating which would shield the crystals from mechanical stresses. The slurry coated models used in the present study were coated with Krylon plastic spray over the ELC. This method provided a hard model surface which showed no airflow shear effects. Although reflections from the light sources are evident, color changes due to temperature were visible in color photographs over the entire model surface.

The rough appearance of the model surface in figure 5 (b,d,f and h) was caused by the method of Krylon spraying used, and the model boundary layer was not affected in any way.

A representative comparison of the temperature profiles obtained from the two types of model coatings is shown in figure 6. While the patterns are generally the same on both models, the line of constant temperature are much clearer on the slurry coated model (fig. 6 b). Broken and nonuniform color patterns on figure 6a were caused by the paper mounting separating from the model as mentioned previously. Clearly defined regions on the slurry coated model (figure 6 b) show the bow shock from the fin and a high temperature region between the bow shock and the fin.

Figures 7 through 10 present temperature profiles on the 14 x 16 in. flat plate (model C) with the shock generator fins at a deflection angle of 15 deg. Color photographs from which the temperature profiles were derived show boundary layer tripping occuring at the higher Reynolds number. This tripping was the result of leading edge surface irregularities caused by slight mismatches between the stainless steel leading edge and the plexi-glass test surface.

Bow shock angles from the shock generator fin are shown in the temperature profiles of figures 8 through 10 and are greater than the 48 deg. Shock angle predicted for a 15 deg wedge in Reference 11. The higher shock angles shown on the profiles were caused by the shock generator fin being behind the bow shock from the basic model. Two different flow fields, one from the flat plate and the other from the shock generator fin, intersect to form the flow field producing the temperature profiles. These figures

show that as the fin is moved forward, the initial shock angle decreases until at $X_F = 0$ in., the shock angle is about 50 deg. The initial shock angle from the fin is also greater for the lower Reynolds number case. A comparison of figures 7 and 9 showed that the shock angle was approximately 3 deg. less for the 20 deg. swept fin (B) than for the 0 deg. swept fin (A).

Secondary areas of high temperature are shown close to the fin/plate junction. While no oil flow or surface pressure data are available for these flow conditions on the model, the flow field appears to compare with that discussed in Reference 4, Section IV. A conical corner flow region starts at the plate/fin junction, and vortices emanating from the corner vertex produces regions of separation and reattachment with higher temperatures evident in the reattached regions.

Temperature profiles in the interference region of the model with the fins at 5 deg. deflection are presented in figures 11 and 12 for a Reynolds number of 1.0 million per foot. Predictions from Reference 11 for a 5 deg. wedge show an undisturbed shock angle of about 36.5 deg. Profiles of figures 11 and 12 indicate a minimum shock angle of about 28 deg. for the 20 deg. swept fin (figure 12b) to 37 deg, for the 0 deg. swept fin (figure 11a). As in the profiles for fin deflection angles of 15 deg., the profiles in figures 11 and 12 show secondary areas of high temperature between the fin and bow shock.

Results of using encapsulated liquid crystals on a non-planar surface are demonstrated in the temperature profiles of figures 13 through 16. Reference 7 indicated difficulties in obtaining acceptable results with

12

liquid crystals because of specular reflections and adverse angles of illumination and viewing. On planar models these problems can be resolved by using a single light source and camera placed normal to the model surface. However, on curved surfaces light source and camera placement must be compromised by trial and error. Profiles on the ogive cylinder model presented in figure 13 through 16 indicate very good resolution of fin induced separation and high shear regions can be obtained on bodies of revolution equipped with control canards.

Generally, the temperature patterns are quite similar for all canard deflection angles and model angles of attack. A high temperature region is seen in the location of the canard bow shock. A second high temperature region extends along the canard in a region of high shear. Between the two high temperature areas is a low temperature secondary separation region. Although no oil flow data were obtained, temperature profiles indicate flow characteristics similar to those formed on the flat plate models and results at higher Mach numbers such as presented in References 4 and 12.

The base geometry of canards A and B was contoured to match the surface of the ogive cylinder with a canard deflection angle of 0 deg. As the canards were deflected to 15 deg., a gap appeared between the front point of the canard and the model body. This gap was unavoidable and is especially apparent in figures 13 and 14. At a canard deflection of 0 deg., the color change start is 0.10 to 0.20 in. behind the front of canard A. Small disturbances in temperature profile occuring about the 9.25 in. station were caused by the roll pin used to fasten the canard to the model.

C. Mach 3.00 Data

A very abbreviated test program was conducted in the 2 ft TGF at Mach 3.00 to determine the sutiability of the models and test procedures at higher Mach number. Maximum stagnation temperature in the TGF was limited to 115°F by mechanical constraints. The adiabatic wall temperature was calculated by the equation

$$T_{AW} = \left[\frac{1 + \left(\frac{\gamma - 1}{2} \right) r M_\infty^2}{1 + \left(\frac{\gamma - 1}{2} \right) M_\infty^2} \right] T_O$$

where r = 0.85 for laminar flow and 0.89 for turbulent flow. For Mach 3 flow at a stagnation temperature of 115°F the adiabatic wall temperatures were calculated as 59.8°F for laminar flow and 74.4°F for turbulent flow. While the color change range of the ELC was suitable for Mach 1.89 testing, model surface temperatures at Mach 3 were suspected of being too low to produce color change profiles of an acceptable quality. Representative results of Mach 3 testing, presented in figures 17 through 19, show that good temperature profiles were obtained in the interference regions of the models.

Figure 17 shows temperature profiles on the flat plate model C with fin A at the most forward position and deflected 15 degrees. At Mach 3 there were no evidences of leading edge imperfections causing tripping of the model boundary layer as was observed at Mach 1.89. The fin bow shock angle shown in this figure is approximately 43 deg. Reference 11 predicts

14

a shock angle of 32.2 deg for a 15 deg wedge at Mach 3.0. The greater measured than predicted shock angle was caused by the flow fields from the model and fin intersecting to form a flow field similar to the one discussed in Reference 4, Section IV and earlier in this report. Also shown in this figure are a low temperature separated region and a high temperature, high shear region close to the fin.

Figures 18 and 19 present temperature profiles on model D with canard A. Profiles produced on the non-planar model at Mach 3.0 are quite similar to the Mach 1.89 data. The most notable difference is the Mach 3.0 interference regions are narrower than those on Mach 1.89 data. This is due to the lesser canard shock angle at the higher Mach number. The high temperature, high shear region and the low temperature separation area are evident in figures 18 and 19.

V. CONCLUSIONS

The use of encapsulated liquid crystals was shown in Reference 5 to produce better results than raw liquid crystal for temperature measurements on planar models. While Reference 5 presented results of using paper mounted ELC, the present study shows the ELC in slurry form, sprayed on and oversprayed with a protective plastic coating was the most suitable method of using liquid crystals for aerodynamic testing. No adverse effects from mechanical stresses were noted, and color patterns were not obscured by specular reflections.

Use of encapsulated liquid crystals on non-planar surfaces was demonstrated in this study. Temperature profiles were easily discernible over the whole viewing range of the camera, and high temperature regions were obtained on the surface of the ogive cylinder model greater than 75 deg from normal camera viewing line.

The addition of a technique for cooling and shielding the model from the airstream plus a fast model injection system with time base would provide a means of obtaining transient heating rates using liquid crystal coatings. High speed movie photography would be necessary to observe the formation of color patterns on the model.

Results of the present study have shown that encapsulated liquid crystals provide a useful tool in determining flow patterns and regions of high temperatures on models in supersonic flows. This method will be used in future tests to determine high heating areas on weapons systems externally stored on the underside of an aircraft wing at supersonic speeds. More complete mapping of the high heating regions can be accomplished by this technique than with thermocouples on thin skin models.

REFERENCES

1. Neumann, R.D. and Burke, G.L. "The influence of Shock Wave-Boundary Layer Effects on the Design of Hypersonic Aircraft", AFFDL TR 68-152, Mar 1969

2. Jones, R.A. and Hunt, J.L. "Use of Fusible Temperature Indicators for Obtaining Quantitative Aerodynamic Heat-Transfer Data", NASA TR R-230, Feb 1966

3. Patterson, Jerold L. "Heat Transfer Testing in the AFFDL High Temperature Facility Using the Phase Change Coating Technique", FXG TM 70-12, Aug 1970

4. Schultz, H.D. "Experimental and Analytical Investigation of Temperature Sensitive Paints", AFFDL-TR-72-52, June 1972

5. McElderry, E.D. "Boundary Layer Transition at Supersonic Speeds Measured by Liquid Crystals", FDMG TM 70-3, June 1970

6. McElderry, E.D. "Boundary Layer Transition Mapping at Supersonic Speeds Measured by Liquid Crystals", AFFDL-TM-73-5-FXG, January 1973

7. Klein, E.J. " Application of Liquid Crystals to Boundary Layer Flow Visualization", AIAA 3rd Aerodyanmic Testing Conference, AIAA Paper 68-376, April 1968

8. Klein, E.J. "Liquid Crystals in Aerodynamic Testing", Astronautics & Astronautics, Vol. 6 Nr. 7 July 1968, pp 70-73

9. Fergason, J.L , "Liquid Crystals", Scientific American, 211 (2), August 1964

10. Allen, N.H., "The Two-Foot Supersonic Gasdynamics Facility", AFFDL/FXM, 1 August 1968

11. Ames Research Staff, "Equations, Tables, and Charts for Compressible Flow", NACA Report 1135, 1953

12. Bramlette, T. Taz, "Flow Field, Pressure and Heat Transfer Associated with Small Fins in Laminar Hypersonic Flow", SCL-RR-720339, November 1972

Table I, Test Conditions

Model	Mach Nr.	$Re_\infty \times 10^6/ft$	Po, PSFA	To, °F
A, 8" x 16" Paper Coated	1.89	3.0	1600	100 — 115
B, 8" x 16" Slurry Coated	1.89	3.0	1600	100 — 115
C, 14" x 16"	1.89	3.0 1.0	1600 560	100 — 115 100 — 115
D, Ogive Cylinder	1.89	3.0 1.0	1600 560	100 — 115 100 — 115
C, 14" x 16"	3.00	3.0 1.0	2900 1000	110, 115 110, 115
D, Ogive Cylinder	3.0	3.0 1.0	2900 1000	115 115

Table II, Model Configurations Tested

Mach Nr.	Re∞ X10^6/ft	Model	Fin	X, in.	δ deg	α deg
1.89	3.0	A (8 x 16)	A	0,4,8, off	10	0
1.89	3.0	B (8 x 16)	A	0,4,8, off	10	0
1.89	1.0 & 3.0	C (14 x 16)	A & B	0 4 8 off	5,15 0,5,15 0,5,10,15	0
1.89	1.0 & 3.0	D (ogive-cyl)	A & B		0,5,10,15	0,4,8,12
3.00	1.0 & 3.0	C (14 x 16)	A	off, 0,4,8	5,15	
3.00	1.0 & 3.0	D (ogive-cyl)	A & B		0,10	0,5,10,15

19

a. Model C with Fin A

b. Model A or B with Fin B
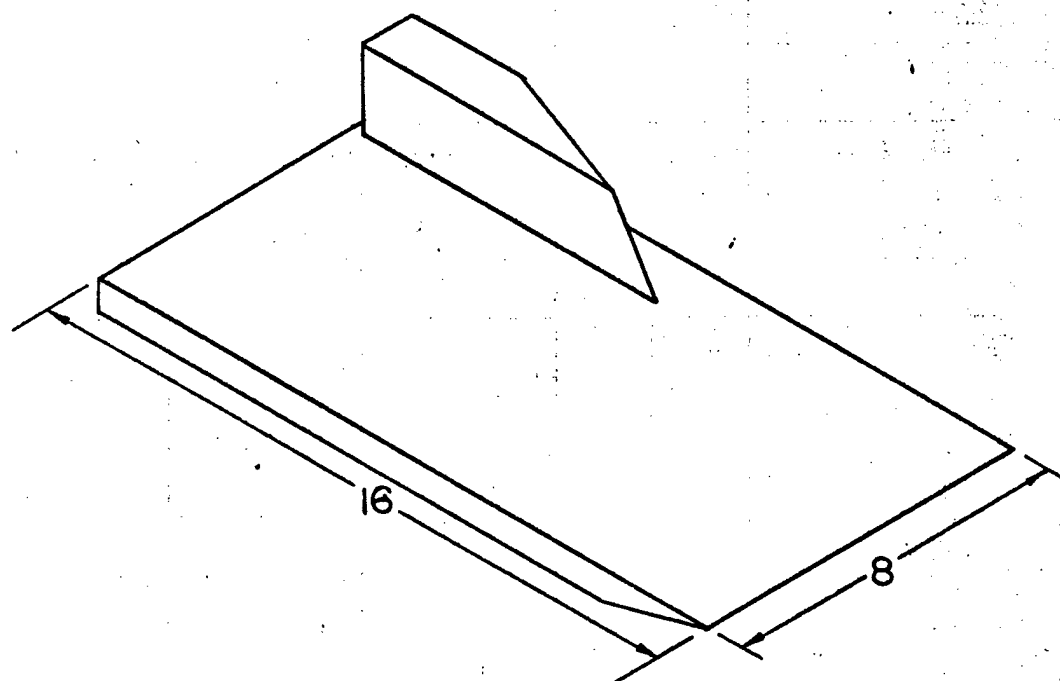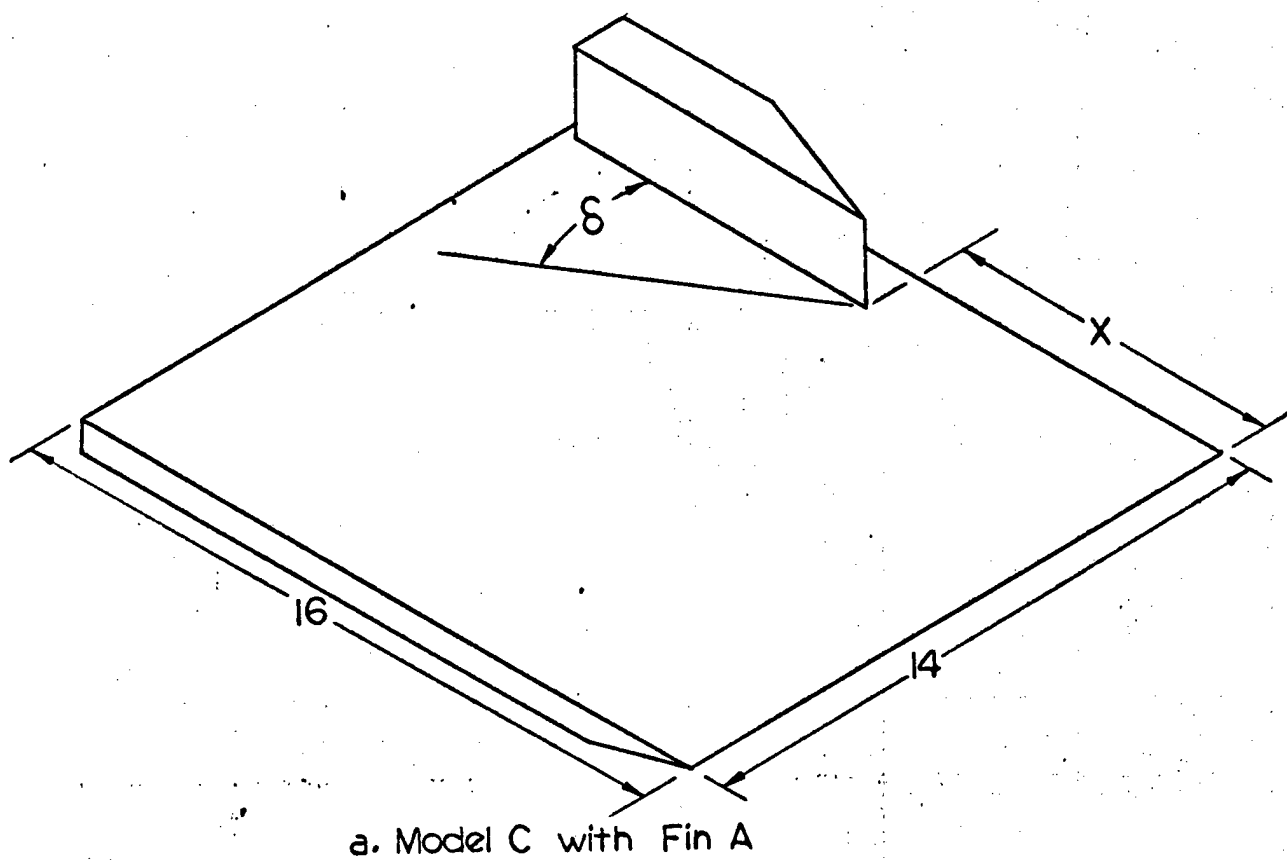
Figure I. Sketches of Flat Plate Models

3.25 Dia.

Canard A

Canard B

12
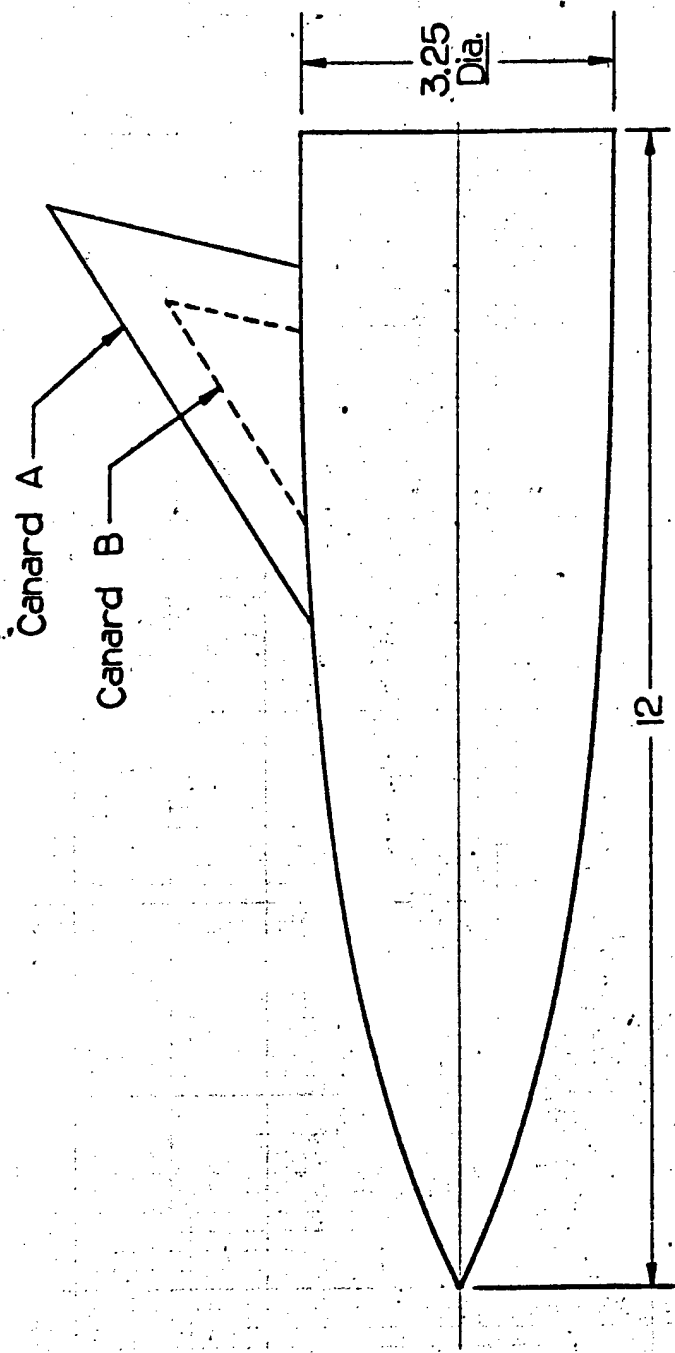
Figure 2. Ogive Cylinder Model D

From Edmund Scientific Co.
Bulletin Nr. 711317-1
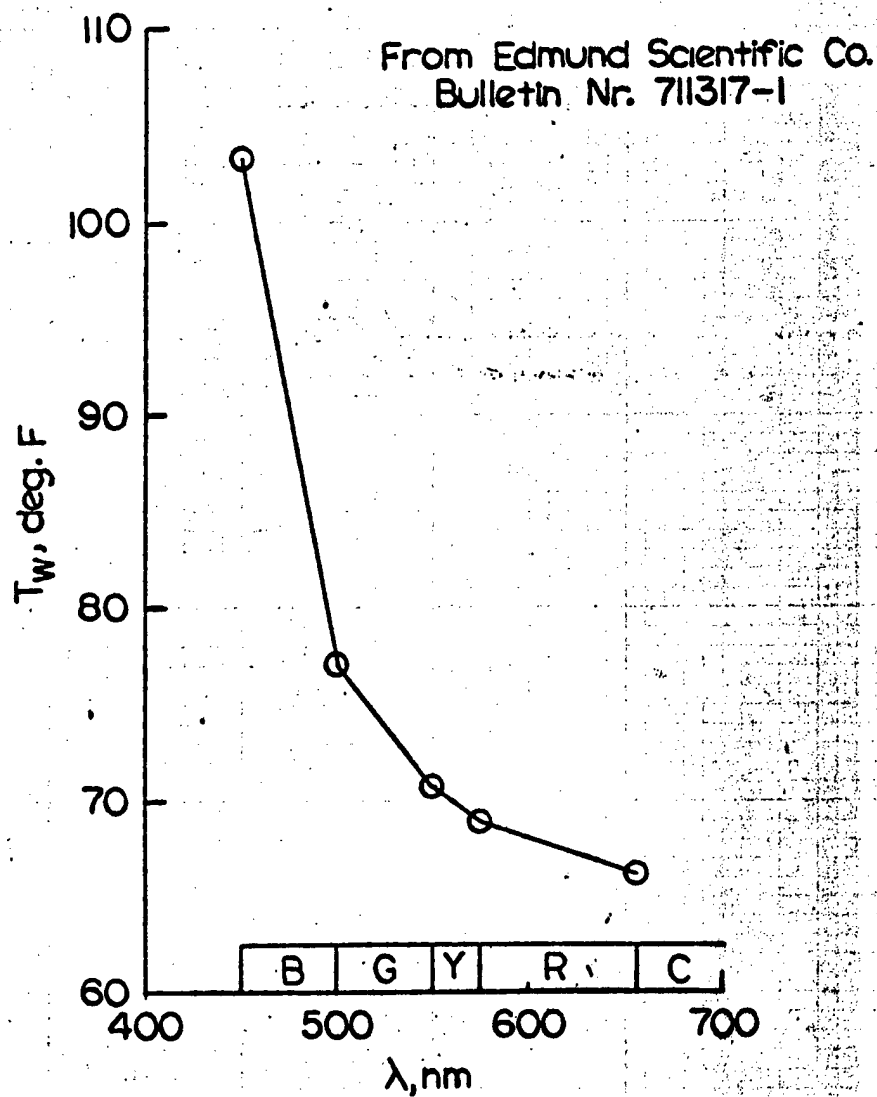
Figure 3. Color-Temperature Variation for NCR Type
W-15 Encapsulated Liquid Crystals

22
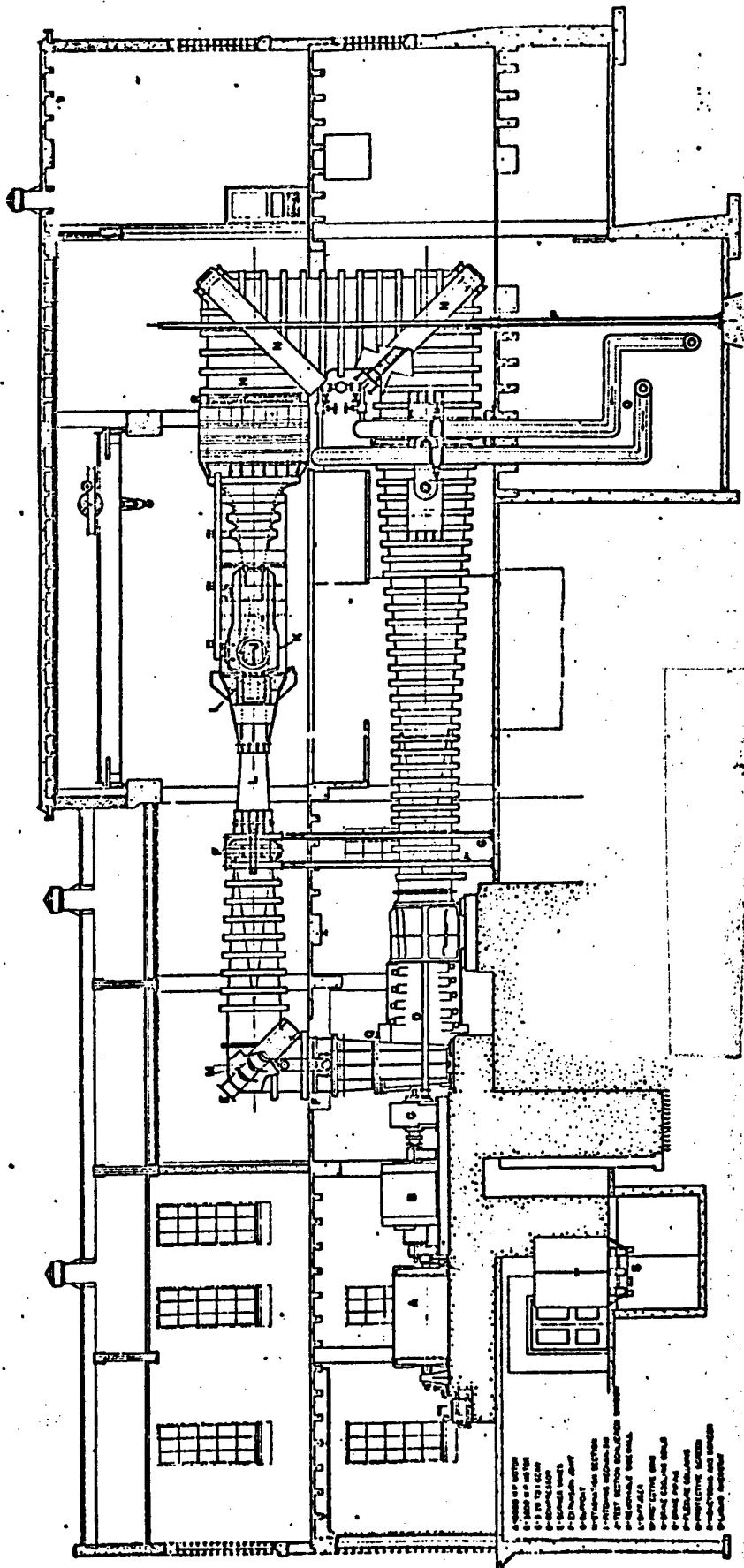
Figure 4. AFFDL Trisonic Gasdynamic Facility

23
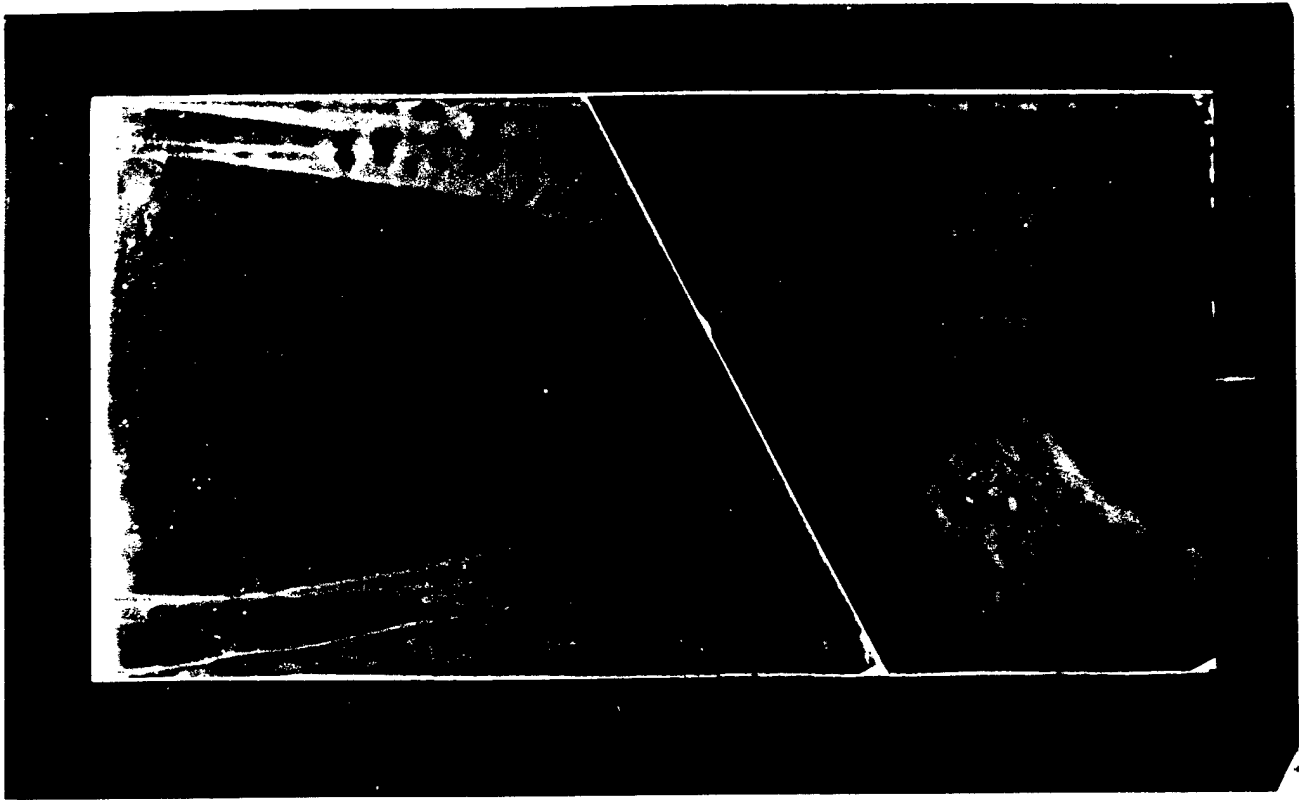
a. Paper Mounting, No Fin
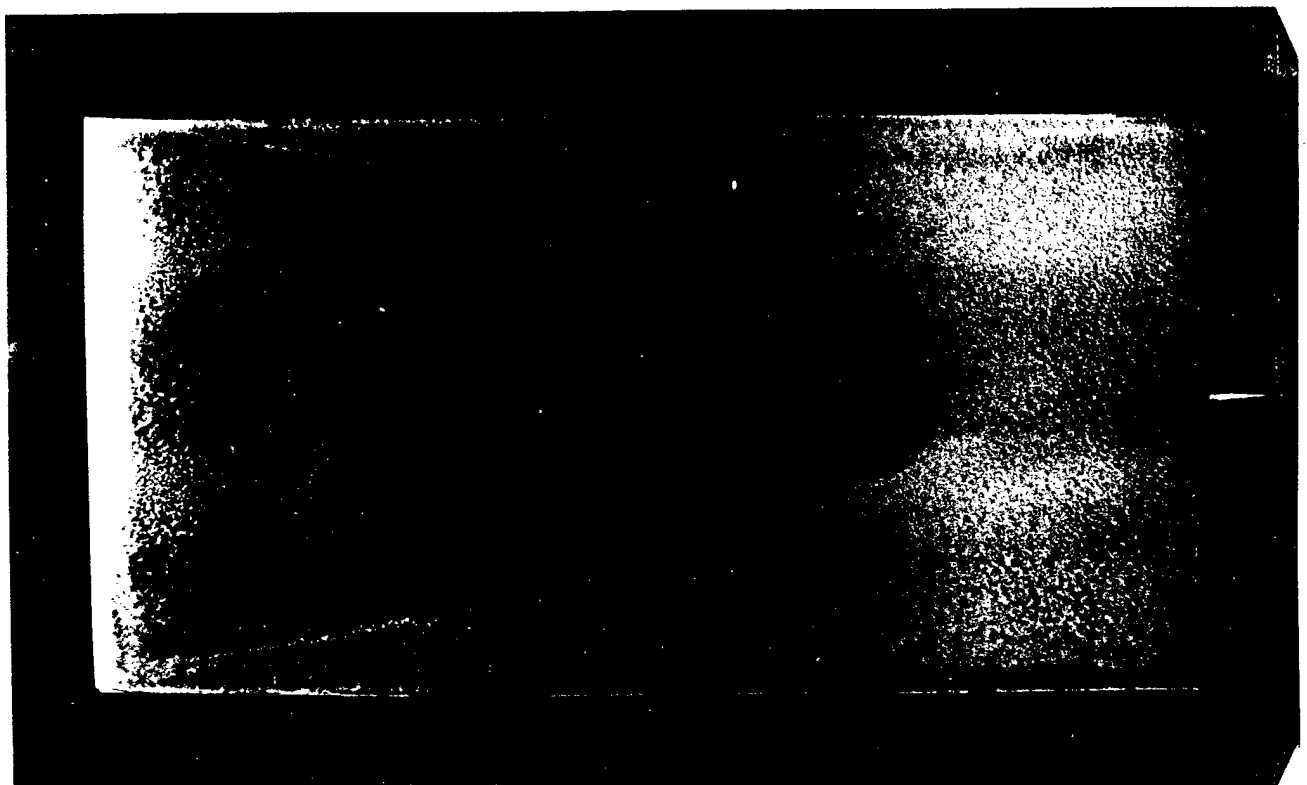
b. Slurry Mounting, No Fin

Figure 7. Comparison of Paper and Slurry Mounting
Methods for Encapsulated Liquid Crystals
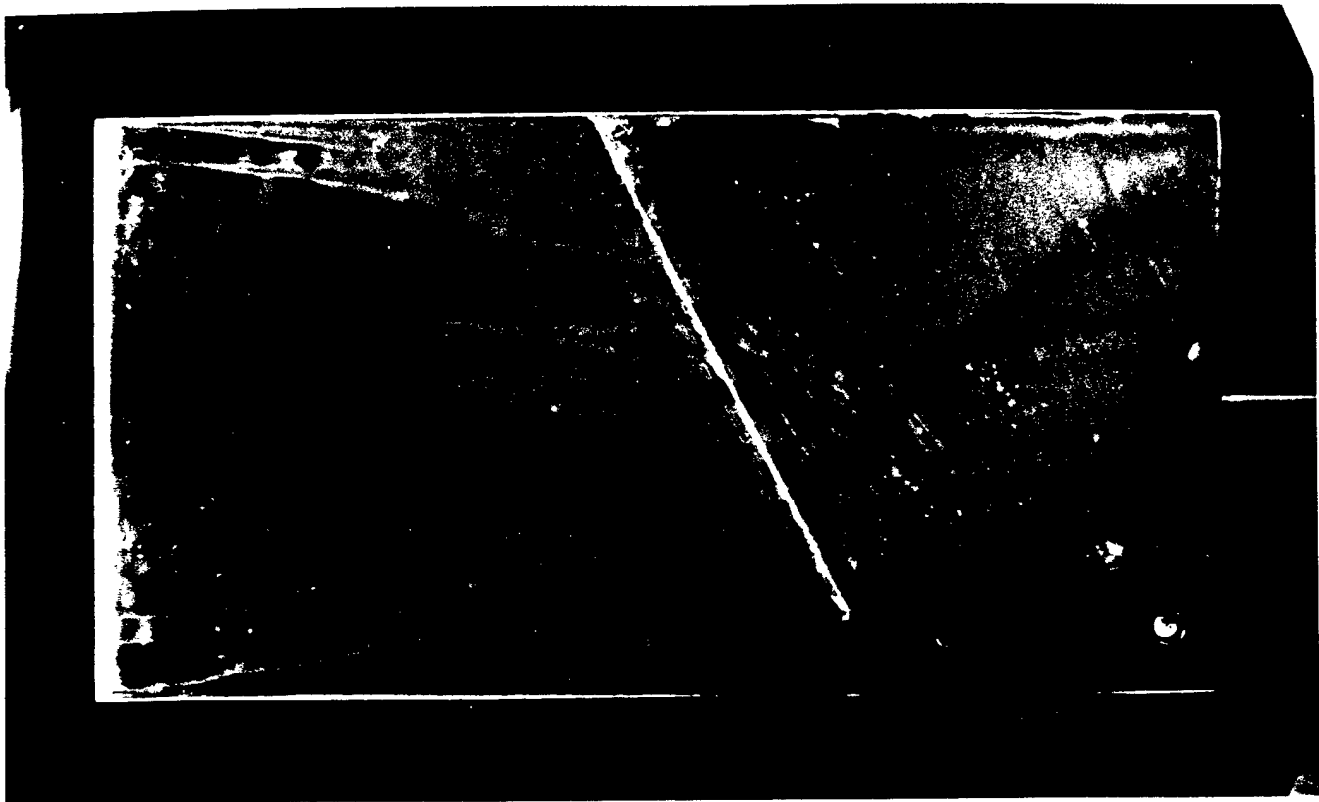
c. Paper Mounting, Fin A, X_F=8in., δ_F=10 deg.

d. Slurry Mounting, Fin A, X_F=8in., δ_F=10 deg.
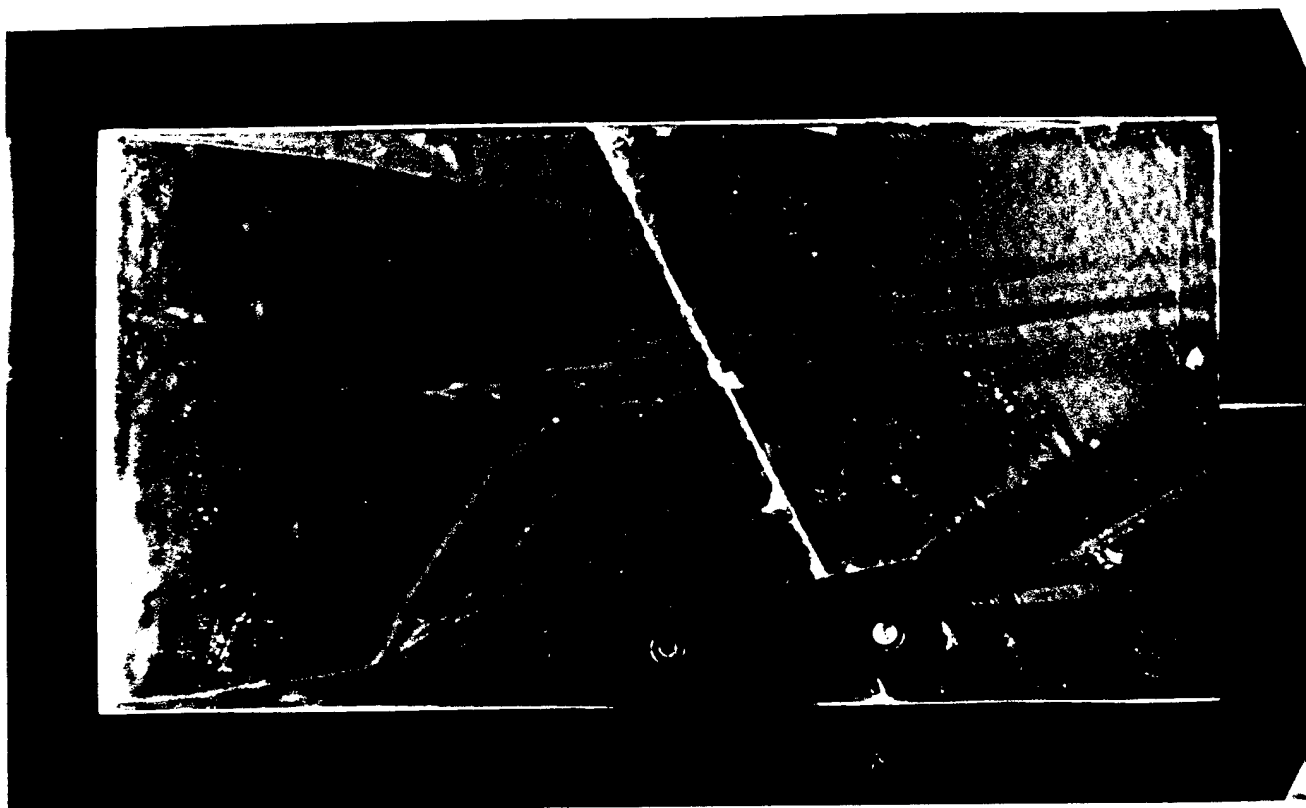
Figure 5. (Continued)

e. Paper Mounting, Fin A, X_F=4in., δ_F=10 deg.
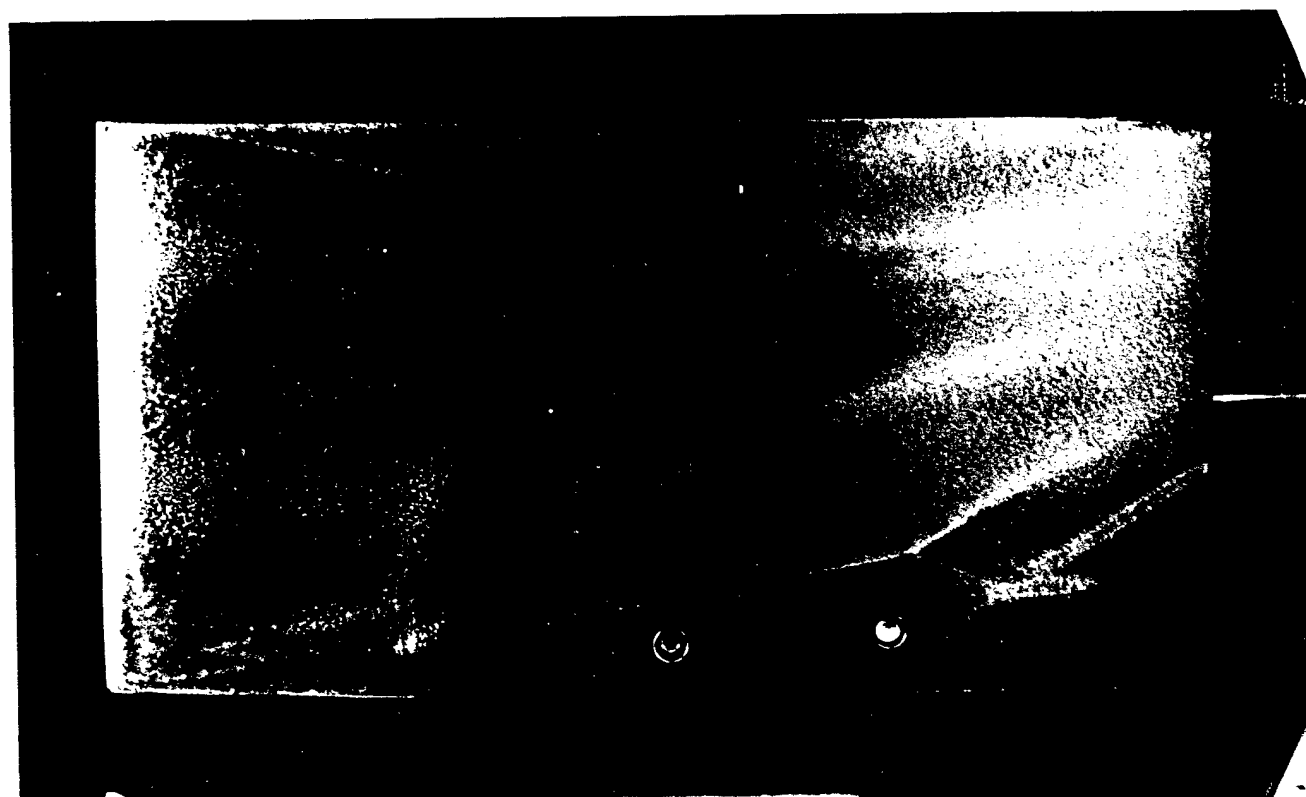
f. Slurry Mounting, Fin A, X_F=4in., δ_F=10 deg.
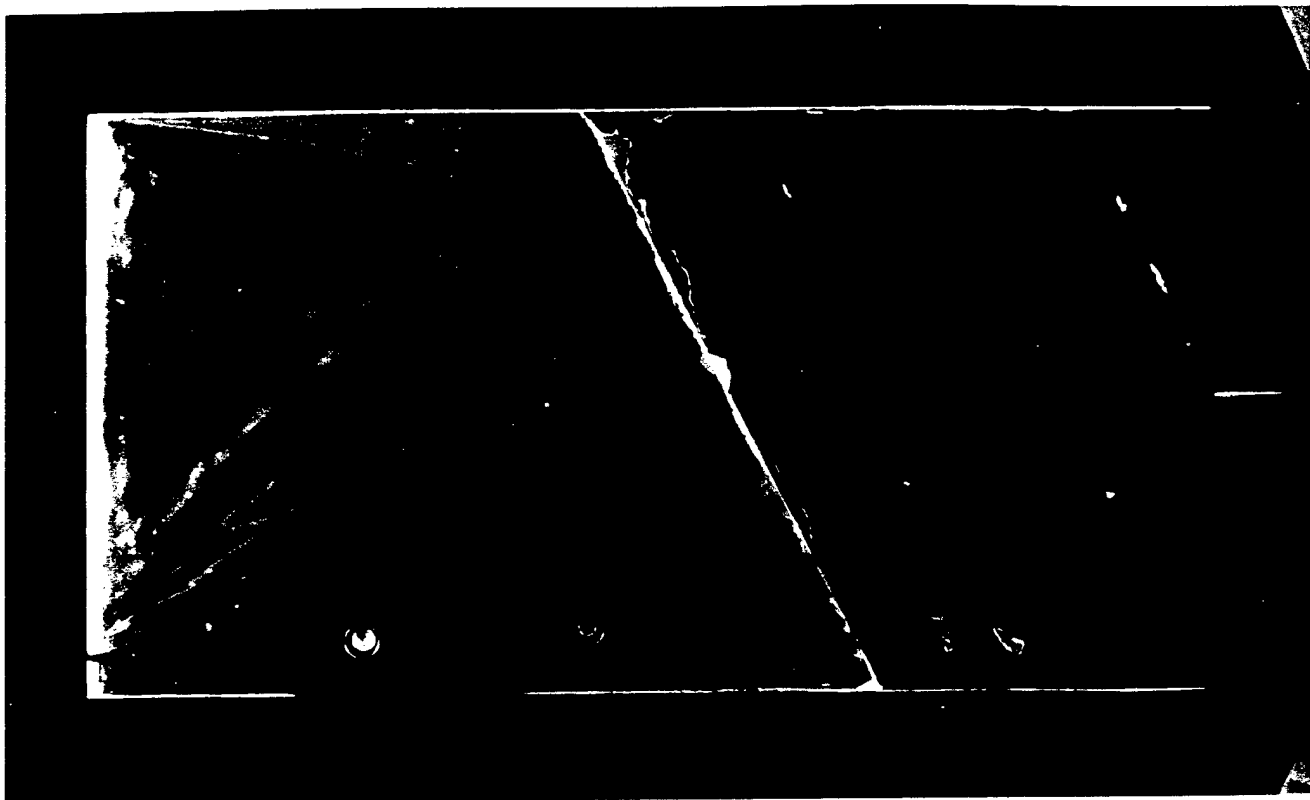
Figure 5. (Continued)

g. Paper Mounting, Fin A, $X_F=0$in., $\delta_F=10$ deg.

h. Slurry Mounting, Fin A, $X_F=0$in., $\delta_F=10$ deg.

Figure 5. (Concluded)
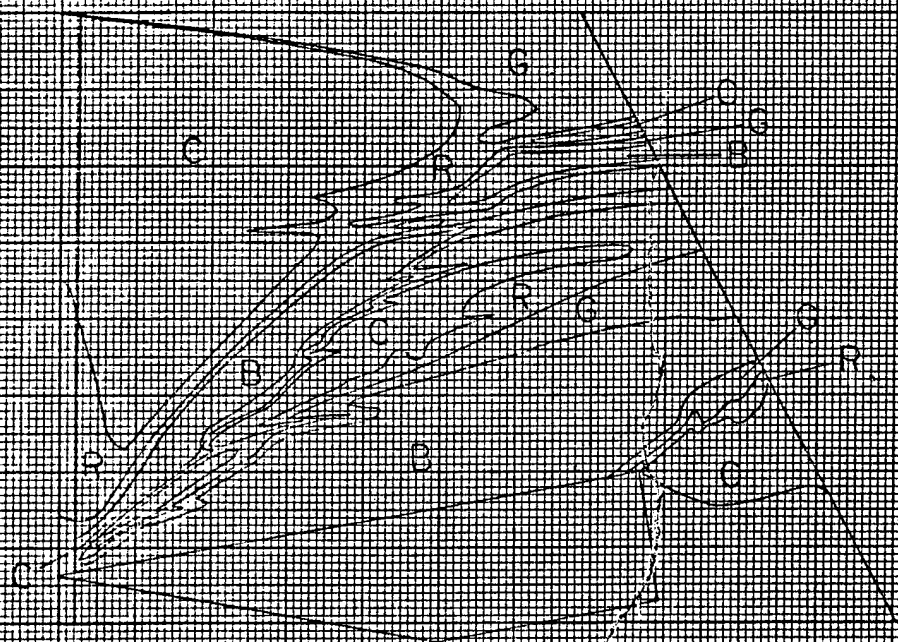
a. Paper Mounting, Fin A, x=-0in, δ=10 deg.

b. Slurry Mounting, Fin A, x=-0in, δ=-10deg.

Figure 6. Comparison of Temperature Profiles for
Paper- and Slurry- Coated Models

g, Xf. 4n, or Iberg.

Figure 7. (concluded)

Figure 34. Flb A1 (2g) 1.0 X C.57 11

Figure 14. $X = 14$ in $6 \tau = 15$ sec.
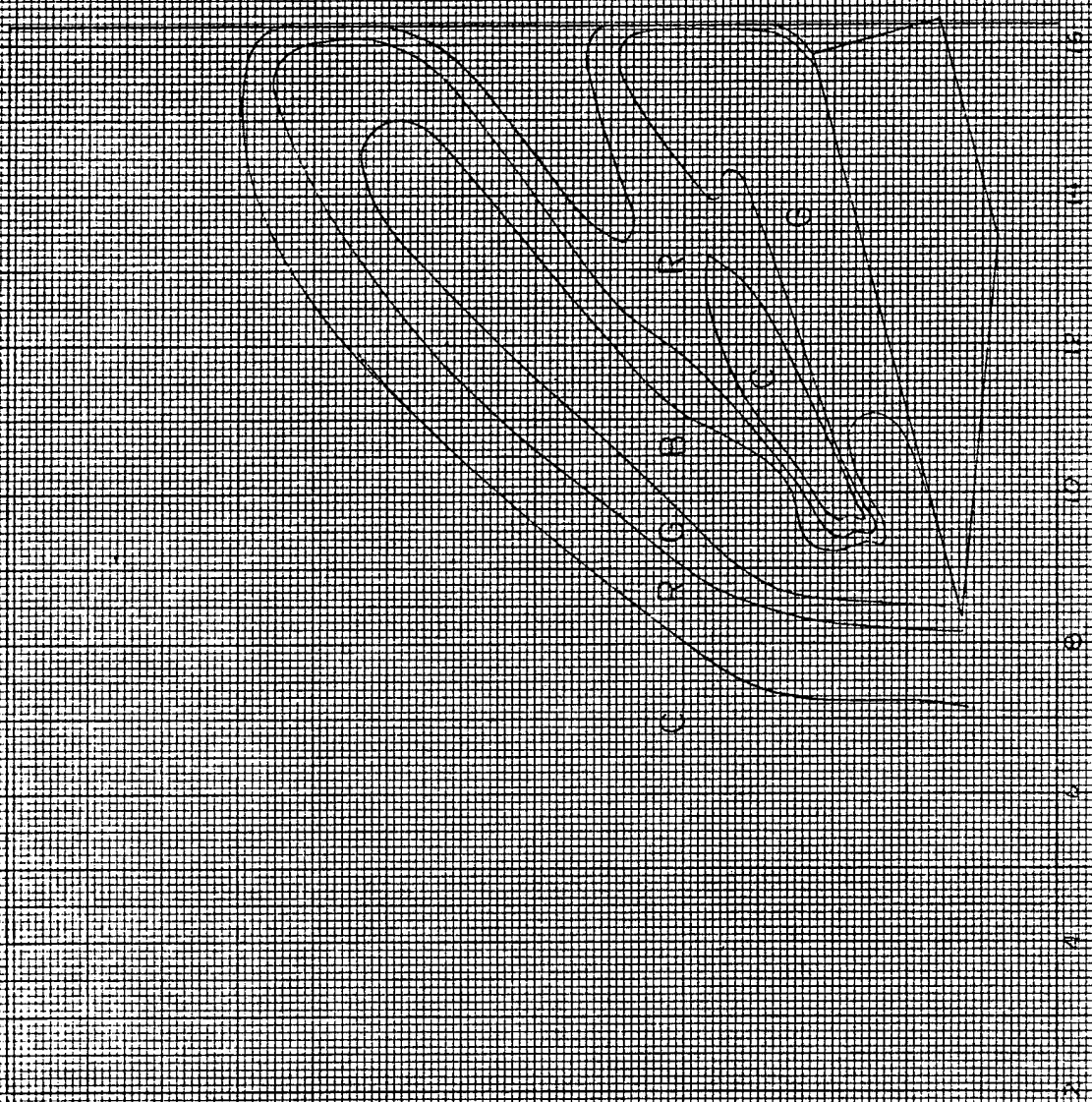
Figure 14. (continued)
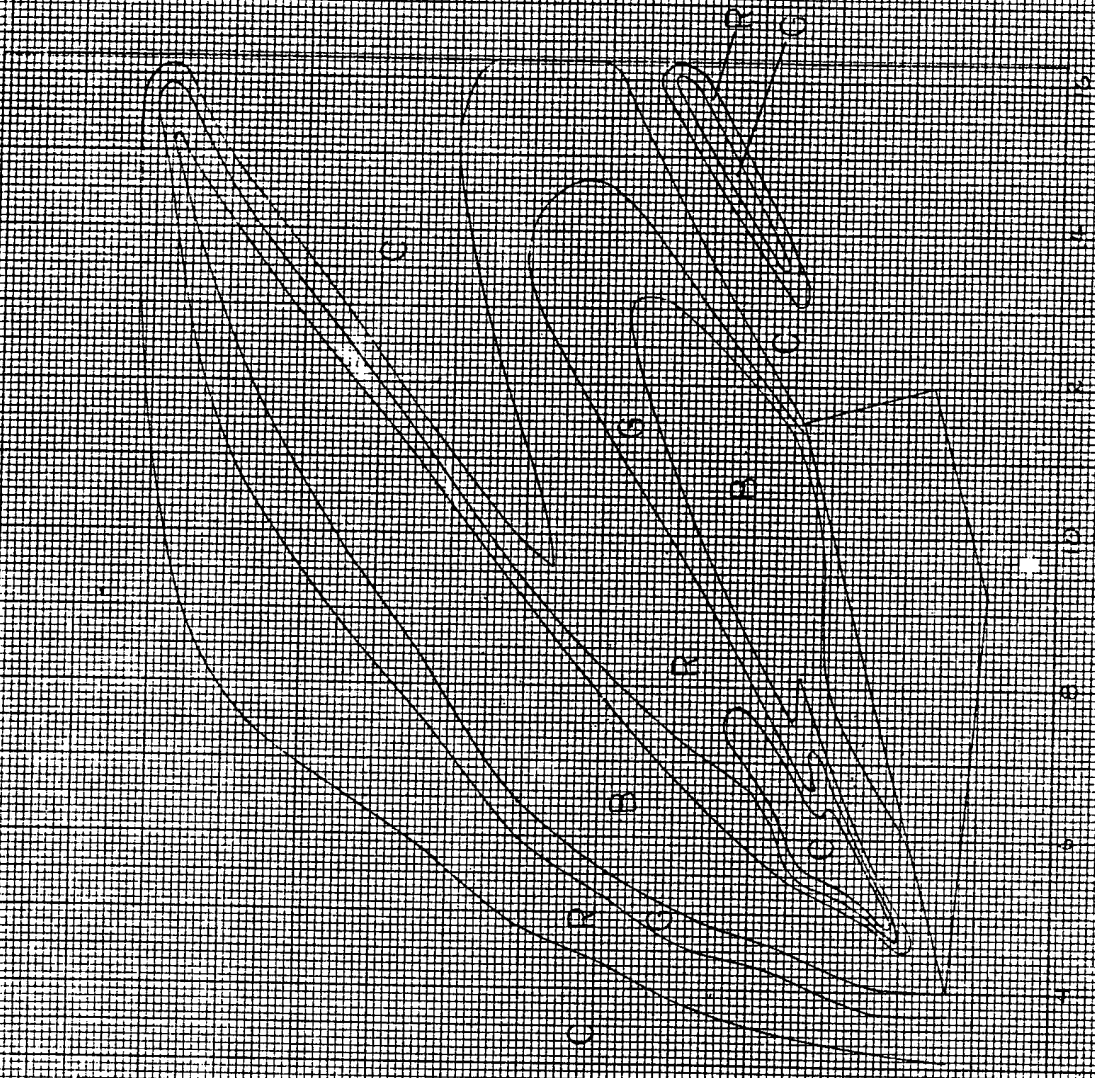
CNE-40 Scribner
Figure 8. (Continued)

a. $X_c = 8in$; $C_k = 15$ cfs;

Figure 26. Full flood routing: $Q_{pa} = 3.9 \times 10^5$ ft.
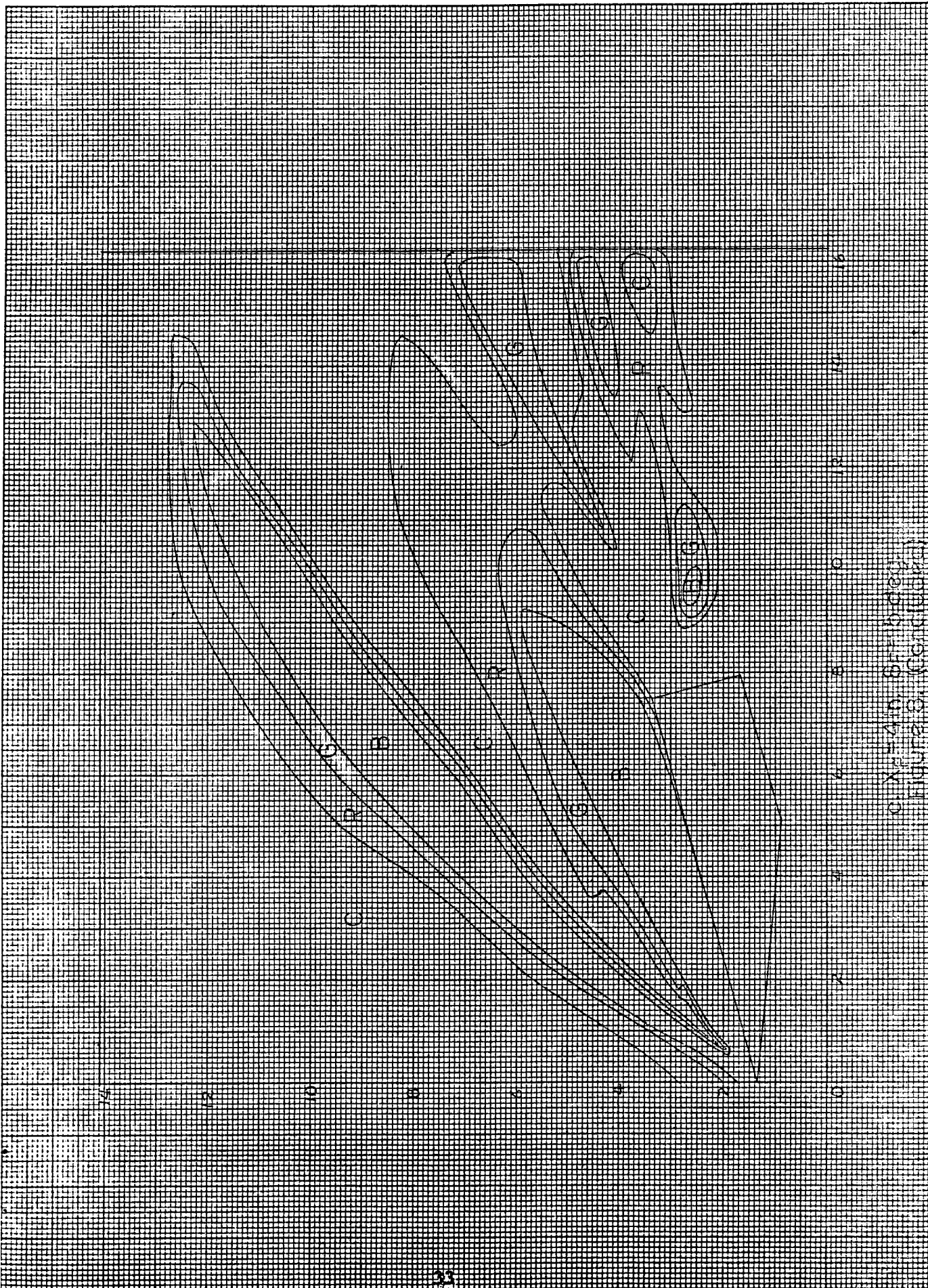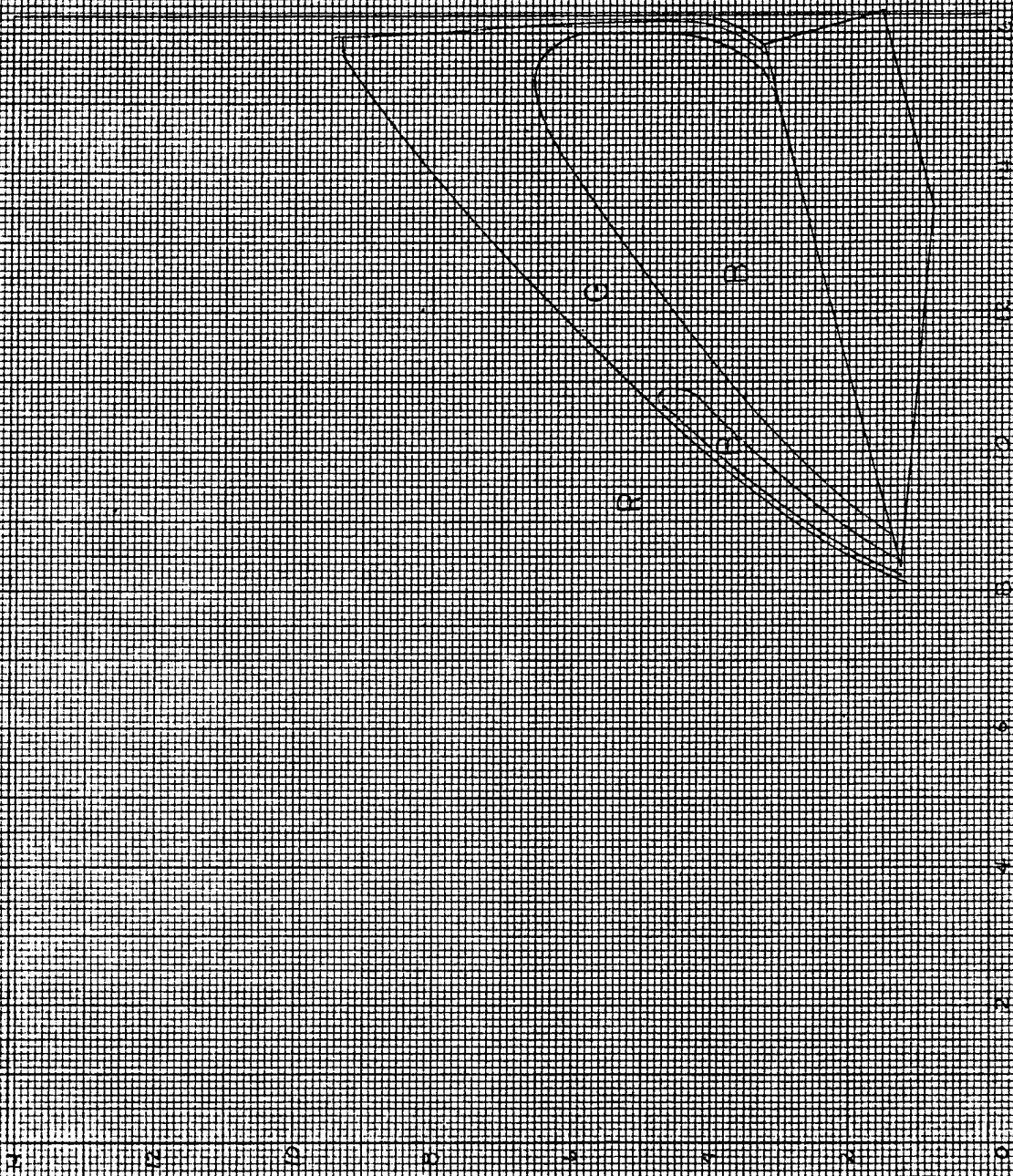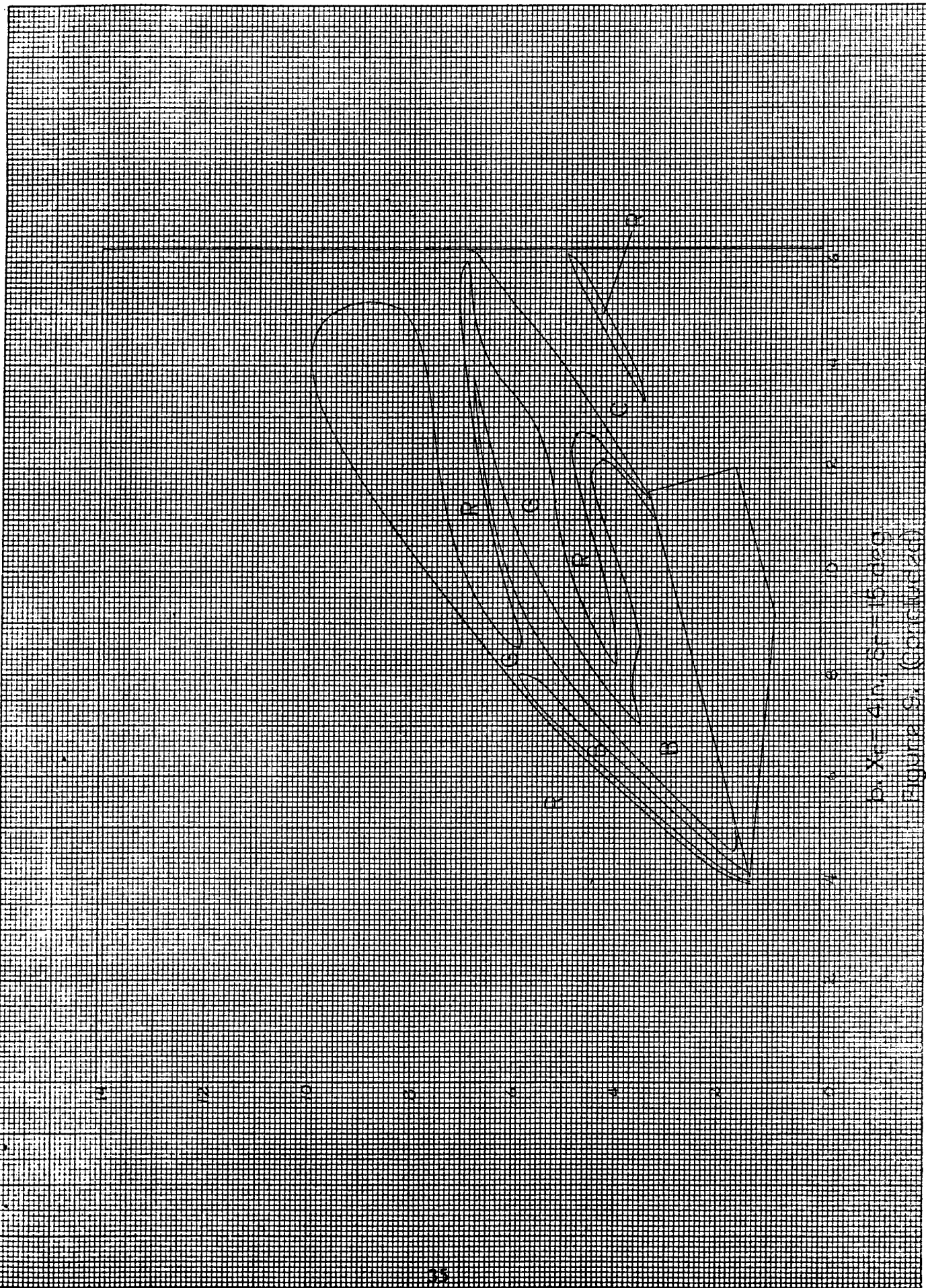
Figure 9. (Continued)

Figure 10. Fn B, beam 10.4MHz SWR

a. Xr = 8in, Sr = 15deg

Figure 12. (Concluded)
b) Xc = 0in. Sy = 5s1g

a. Fin A, α = 0 deg.
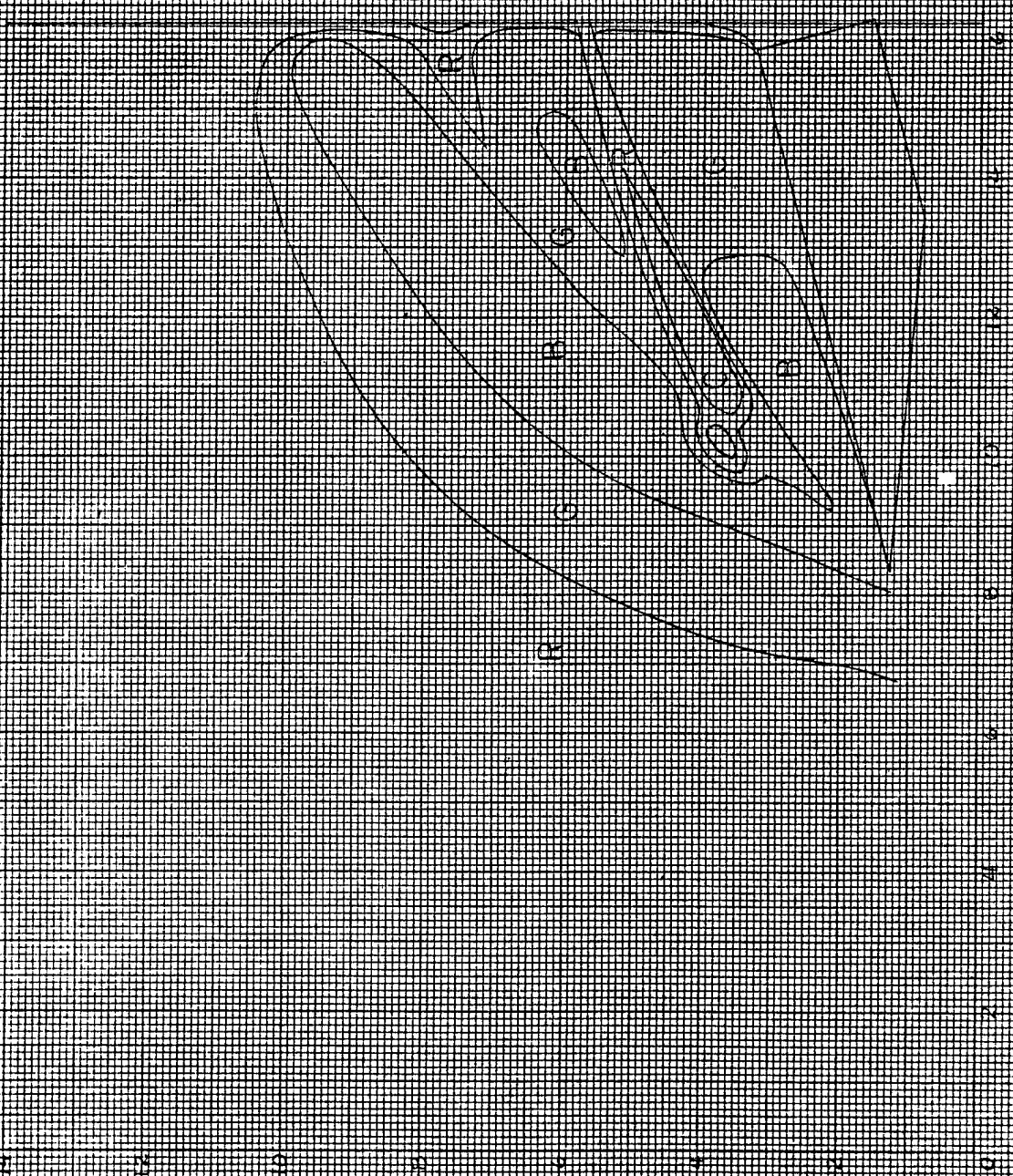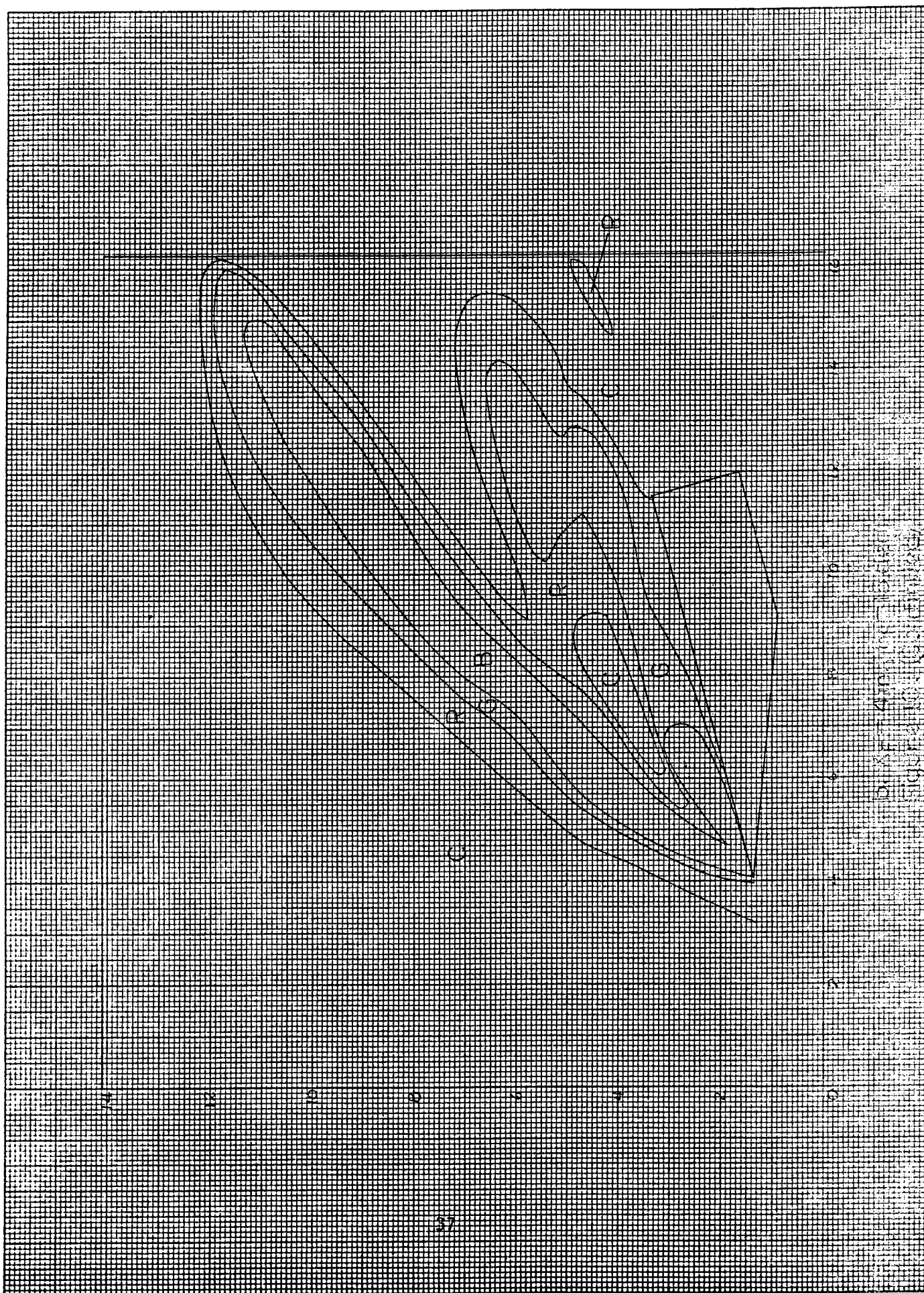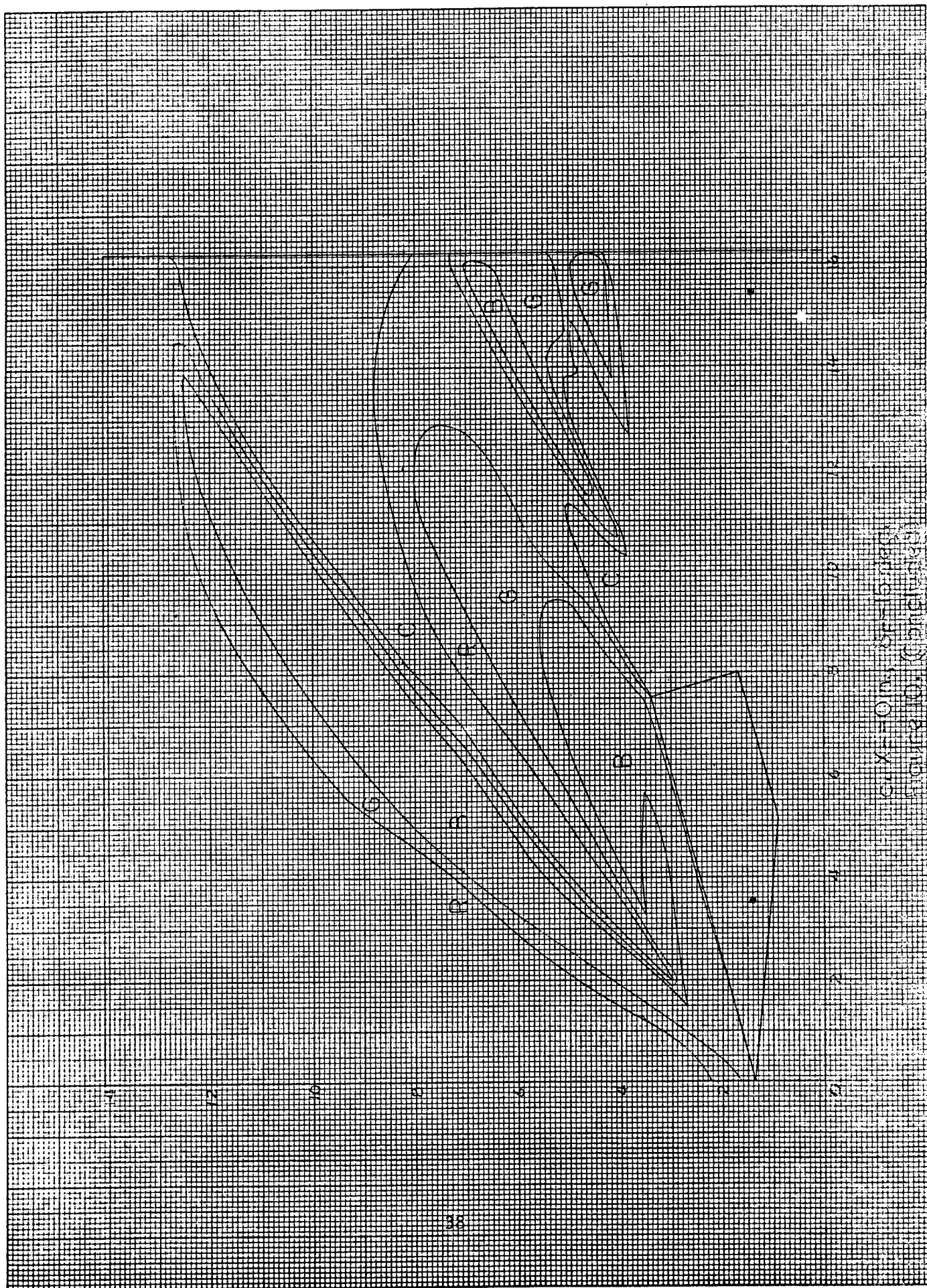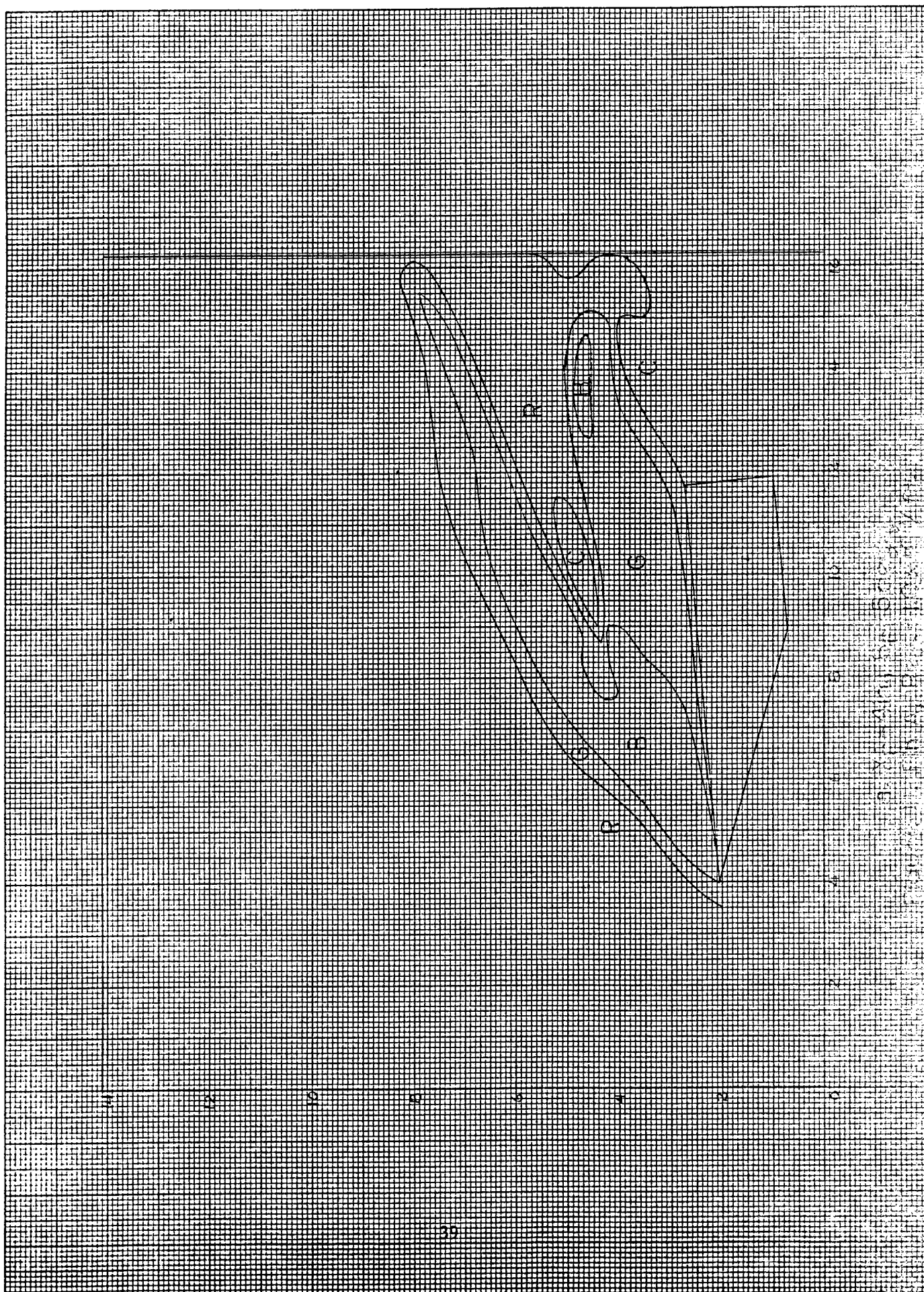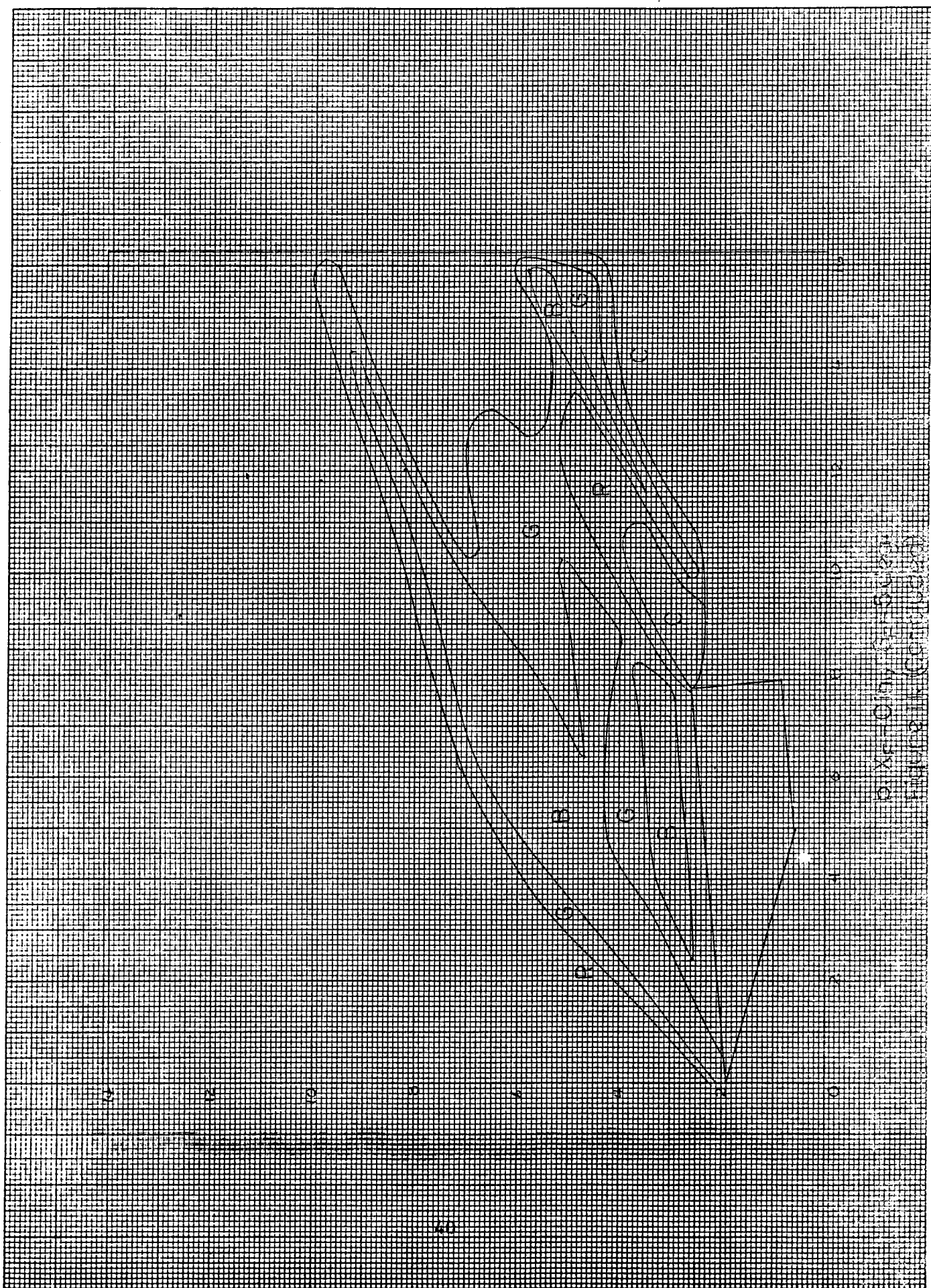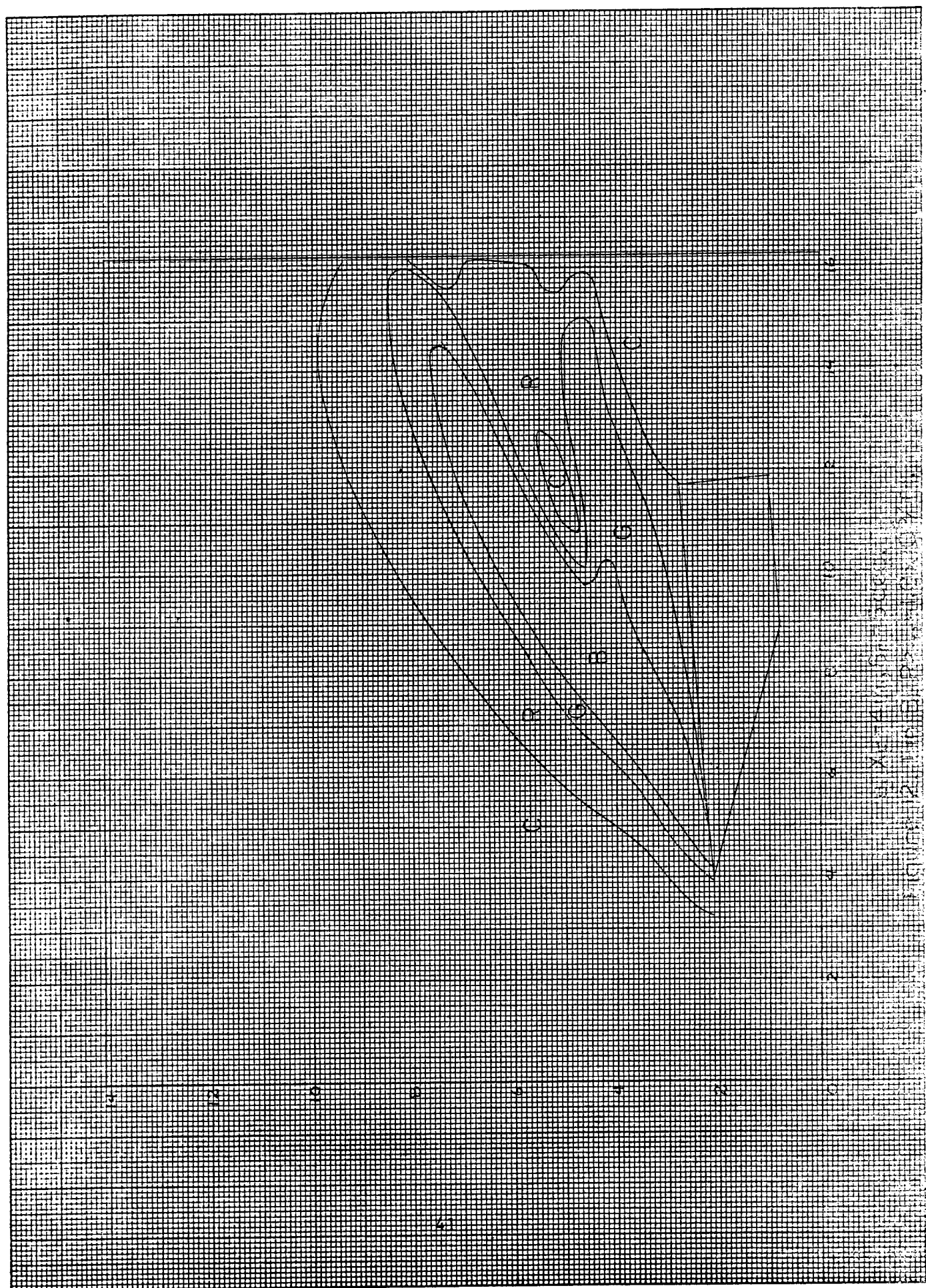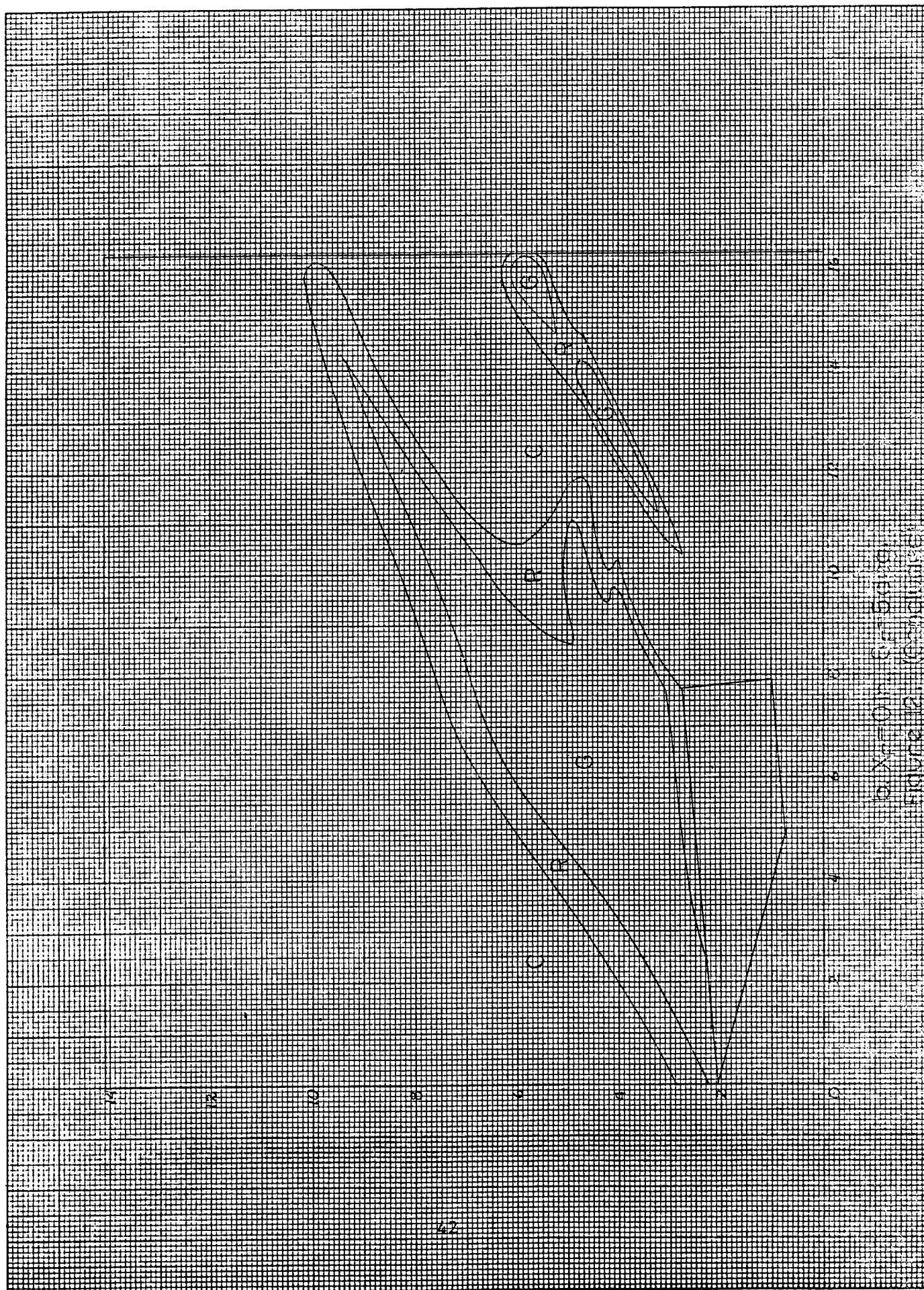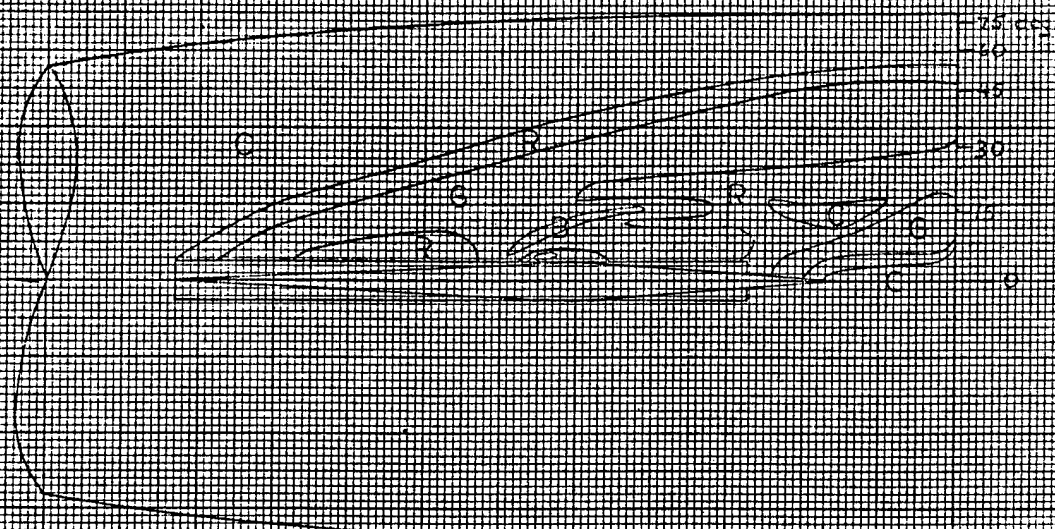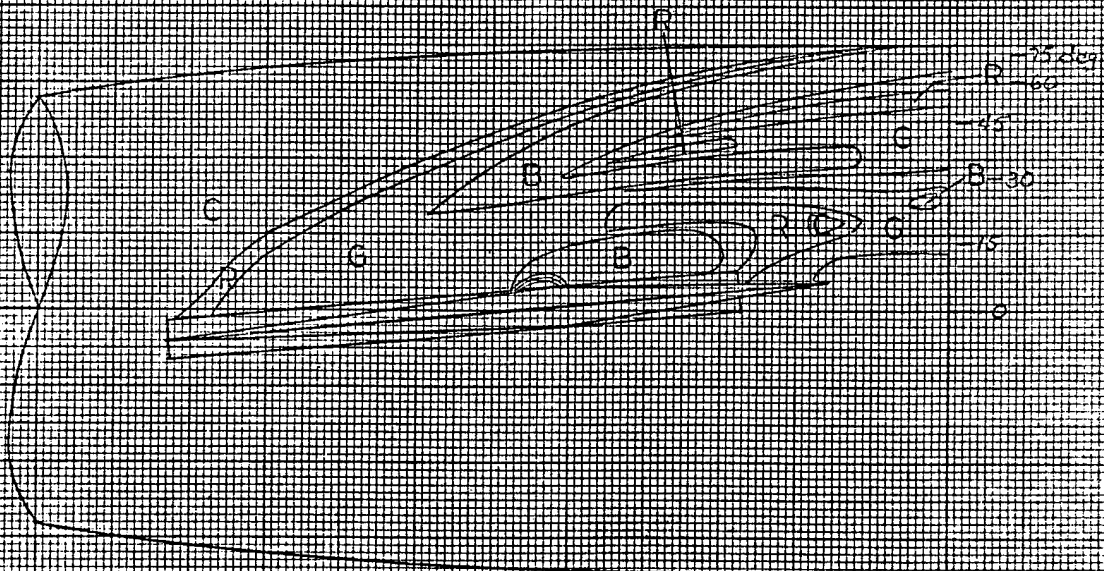
b. Fin A, α = 3 deg.

Figure 3. Temperature Profiles on Model D,
$Re_\infty = 3.0 \times 10^6/ft$, α = 0 deg.

43

c. F in A α = 0 deg.
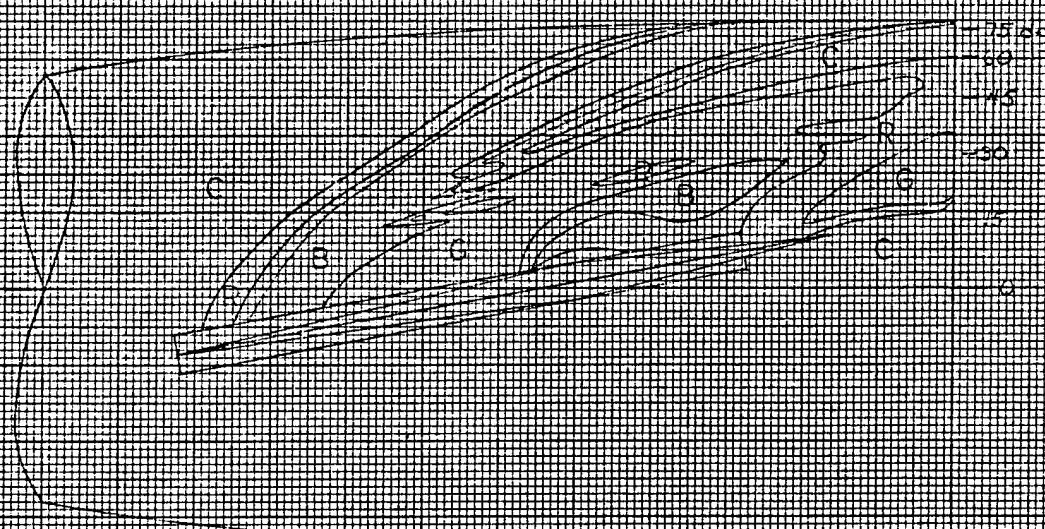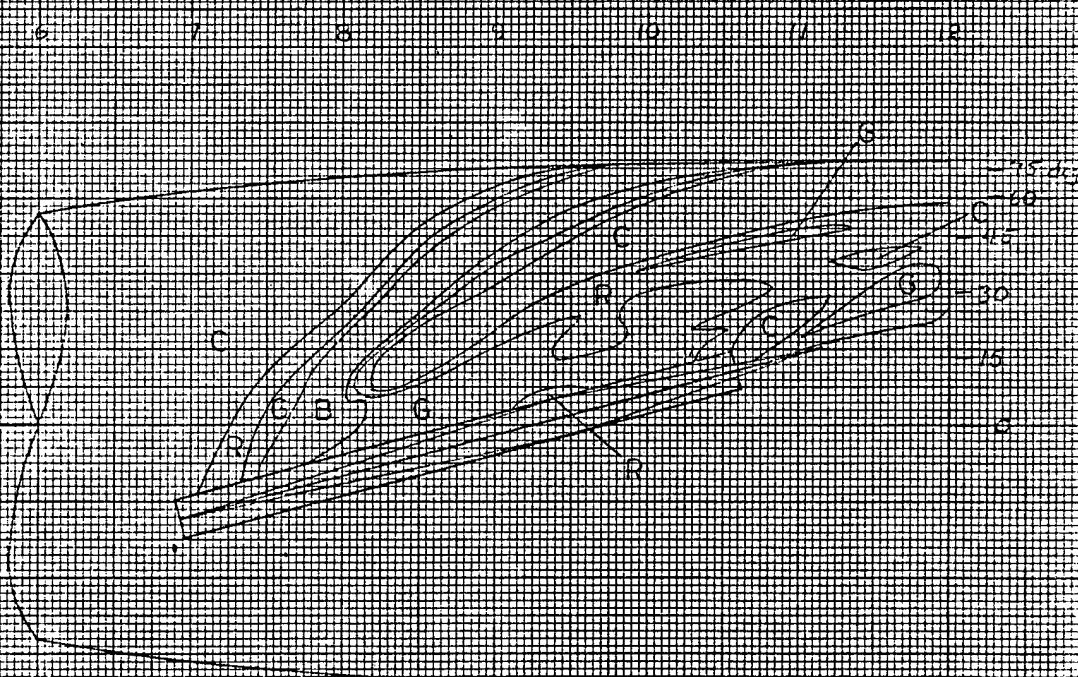
d. F in A α = 5 deg.

Figure 13. (Concluded)

a. Fin A, $\delta_a = 0$ deg.
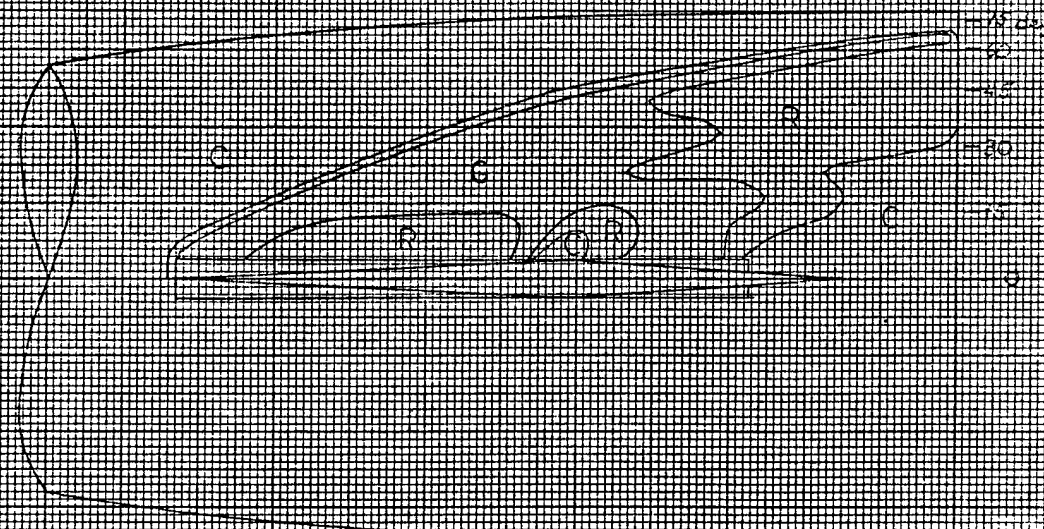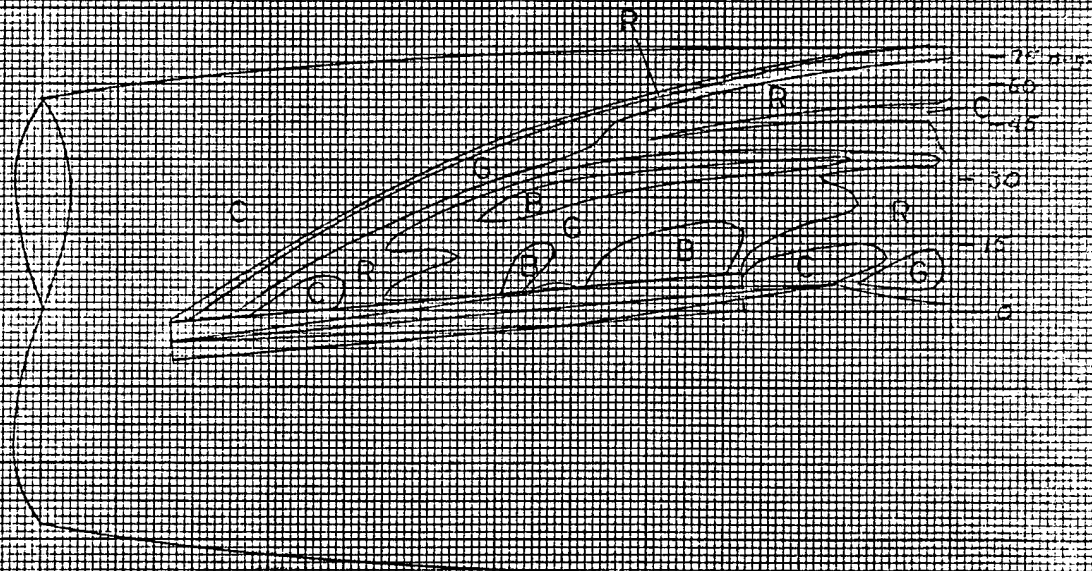
b. Fin A, $\delta_a = 5$ deg.

Figure 14. Temperature Profiles on Model D.
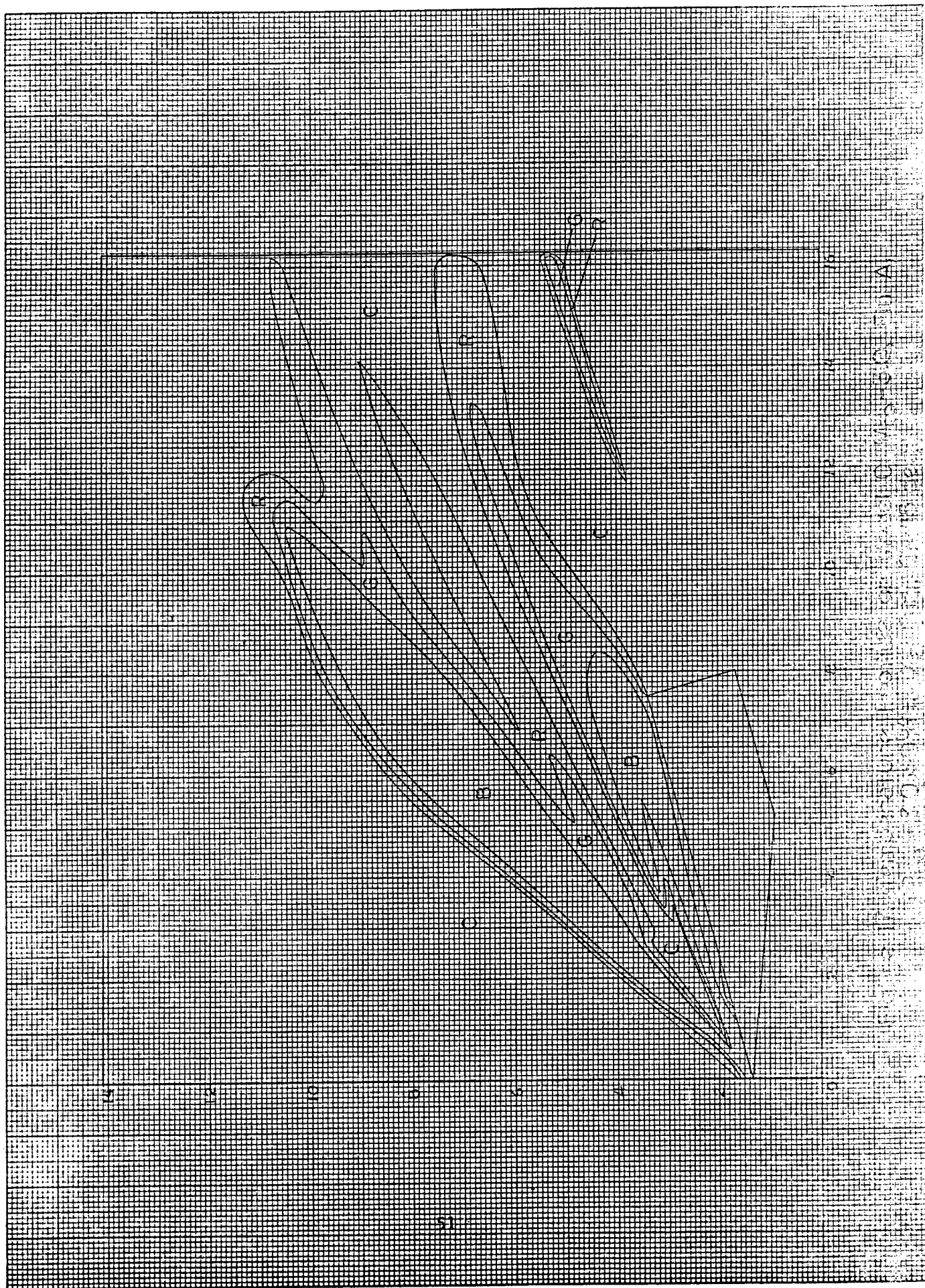$Re_\infty = 3.0 \times 10^6/ft$, $\alpha = 12$ deg.
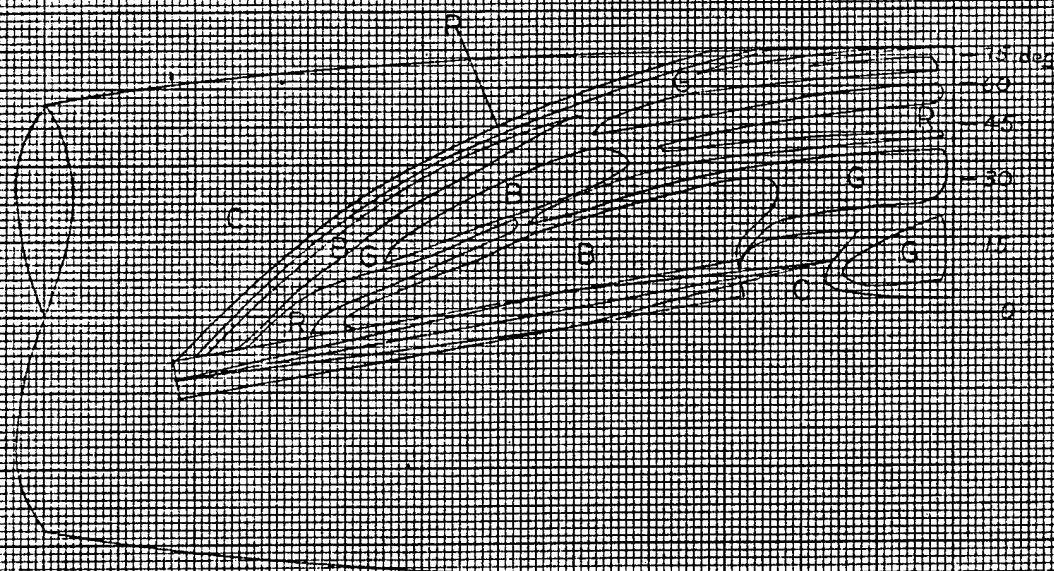
c. Fin A, $\delta_F = 10$ deg

d. Fin A, $\delta_F = -5$ deg

Figure 14. (Concluded)

c. Fr 5, δ=0 deg

b. Fr 5, δ=5 deg
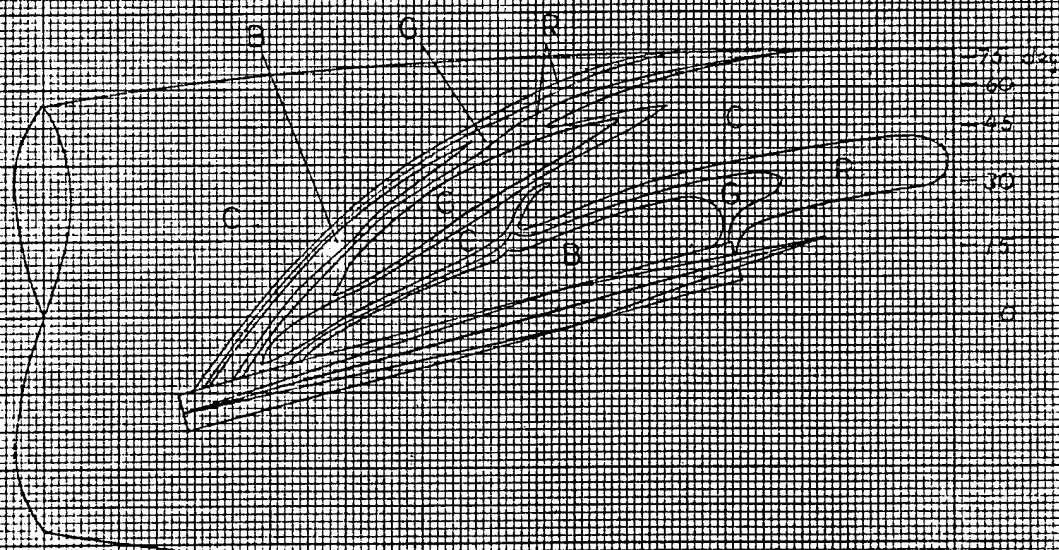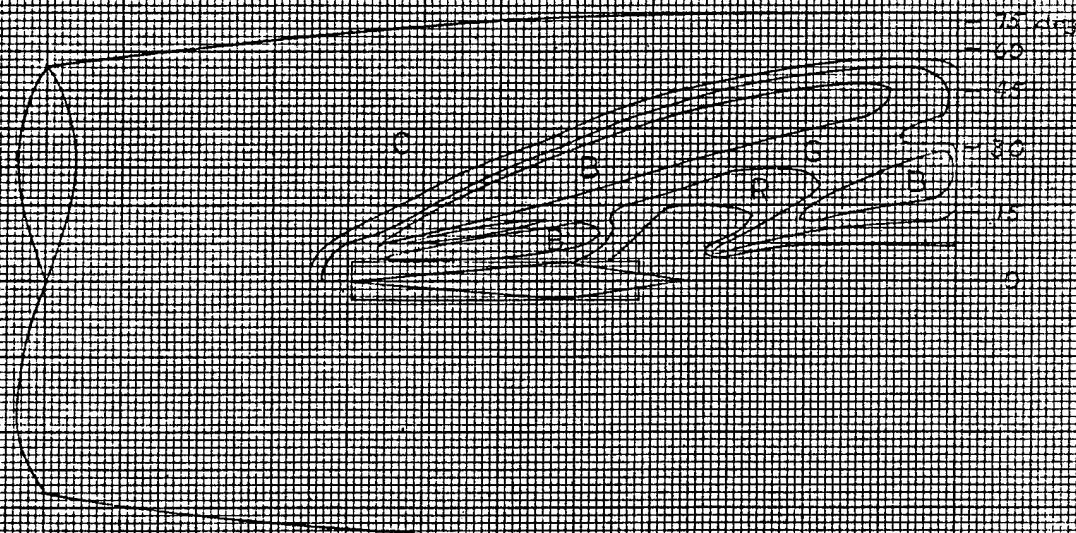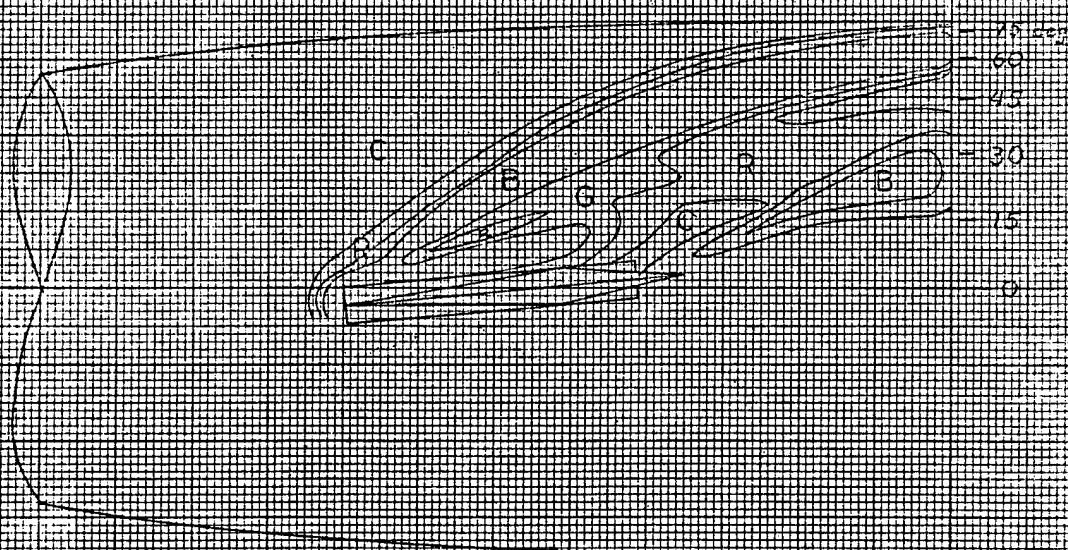
Figure 5. Temperature Profiles on Yacht D.
$Re_\infty = 3.0 \times 10^9$(?), α=0 deg
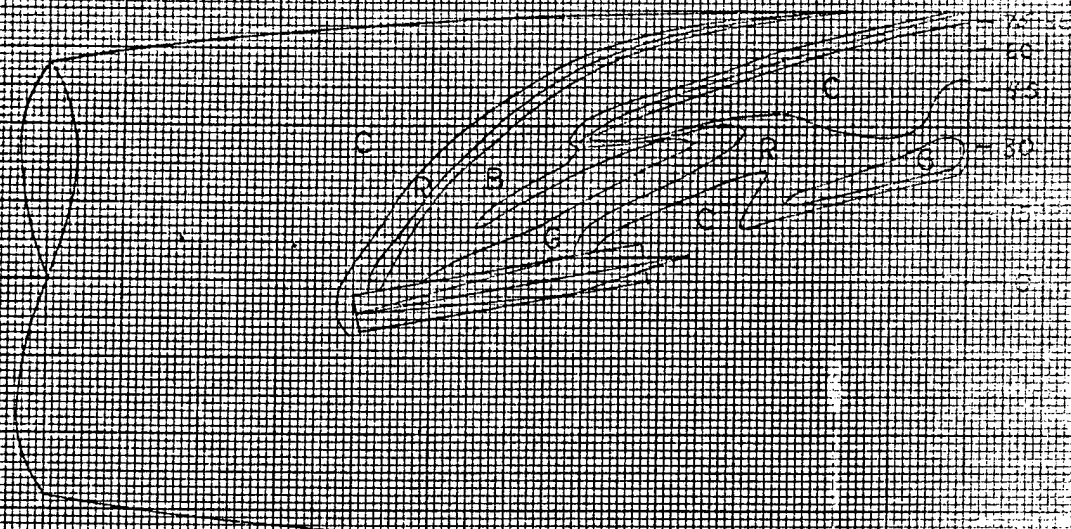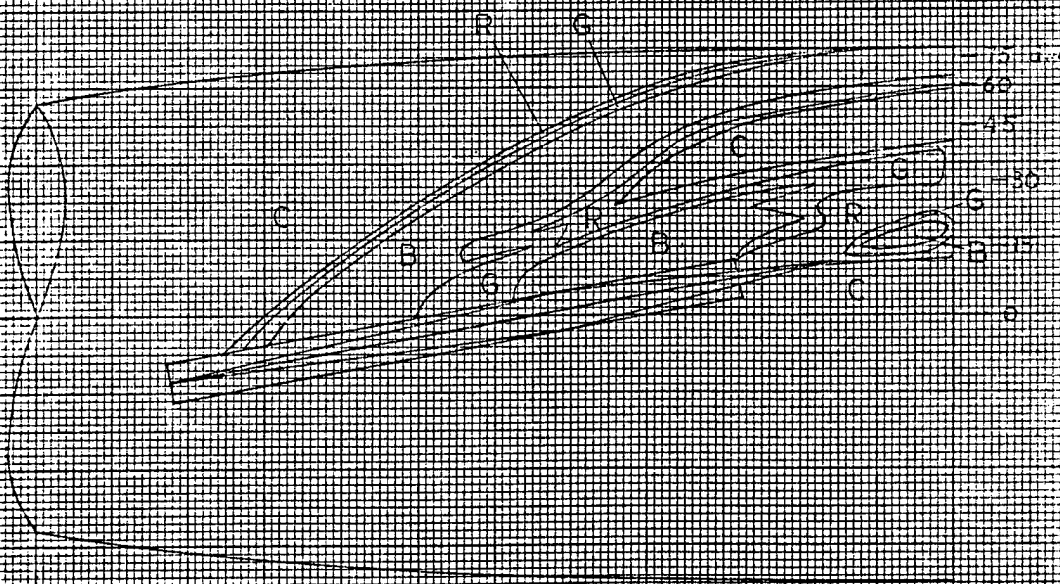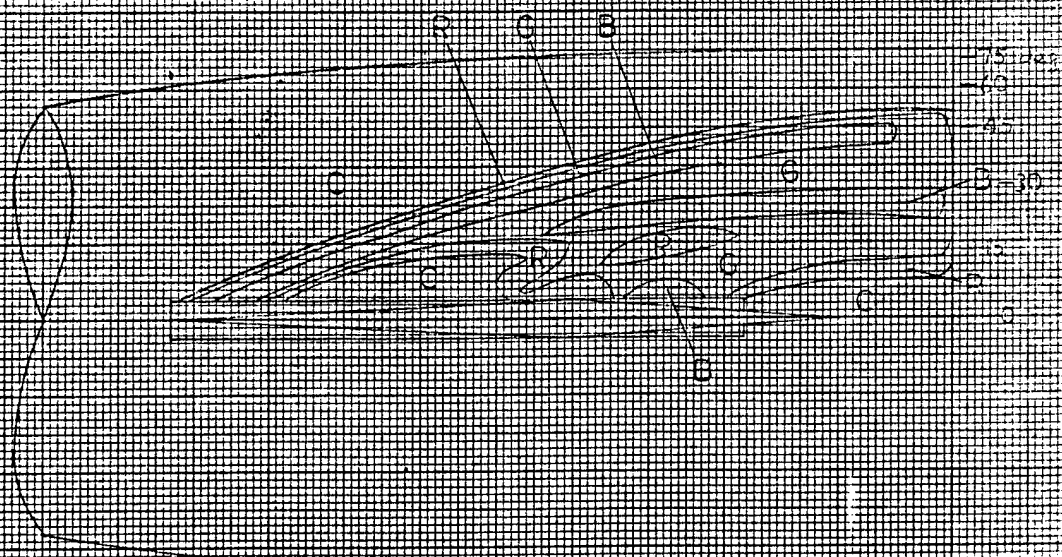
(c) $Fin B; \delta = -10 deg$
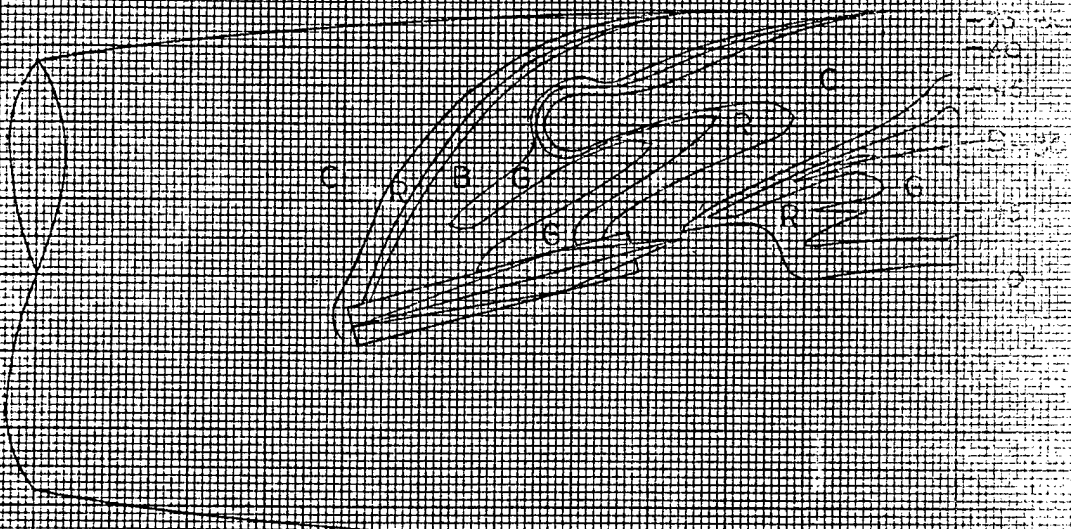
(d) $Fin B; \delta = -5 deg$

Figure 15. (Concluded)

a. Fin B, $\delta_f = 0$ deg.
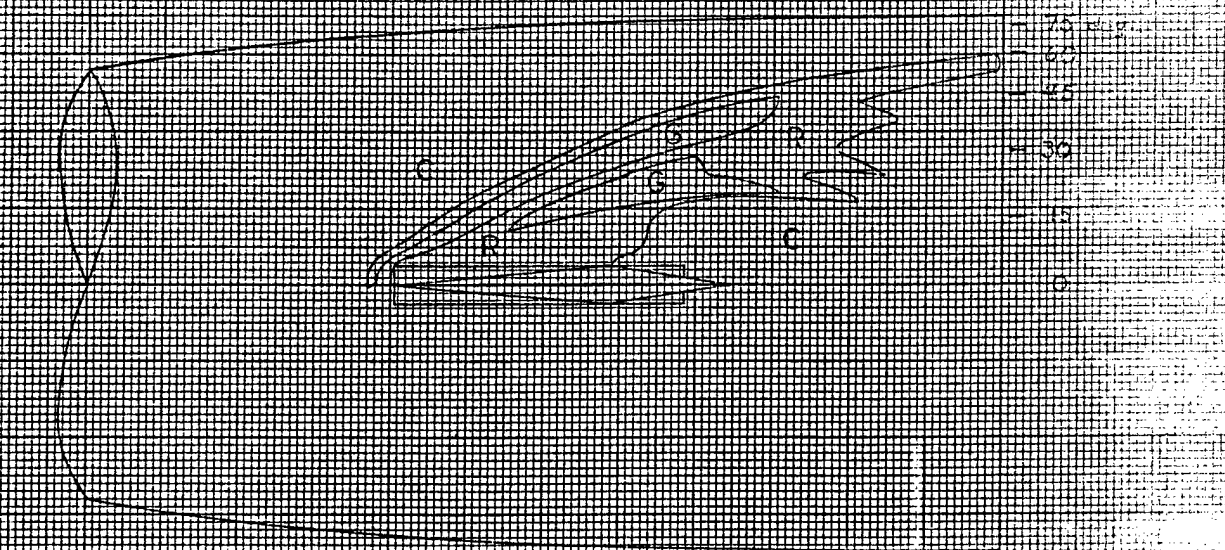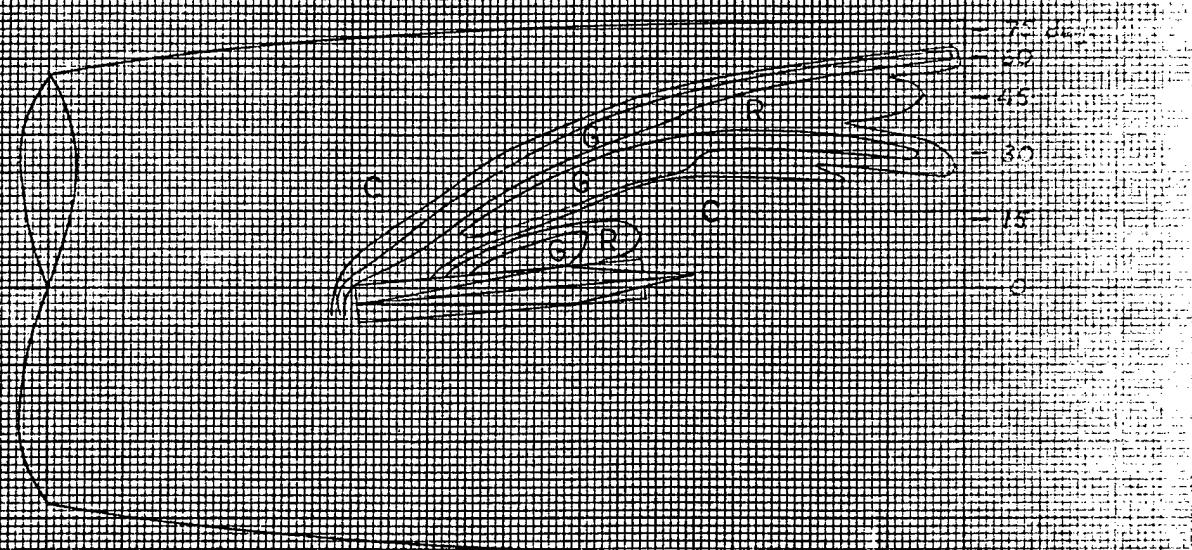
b. Fin B, $\delta_f = 5$ deg.

Figure 2.16. Temperature Profiles on Model D.
$Re_\infty = 3.0 \times 10^6/ft$, $\alpha = 2$ deg.
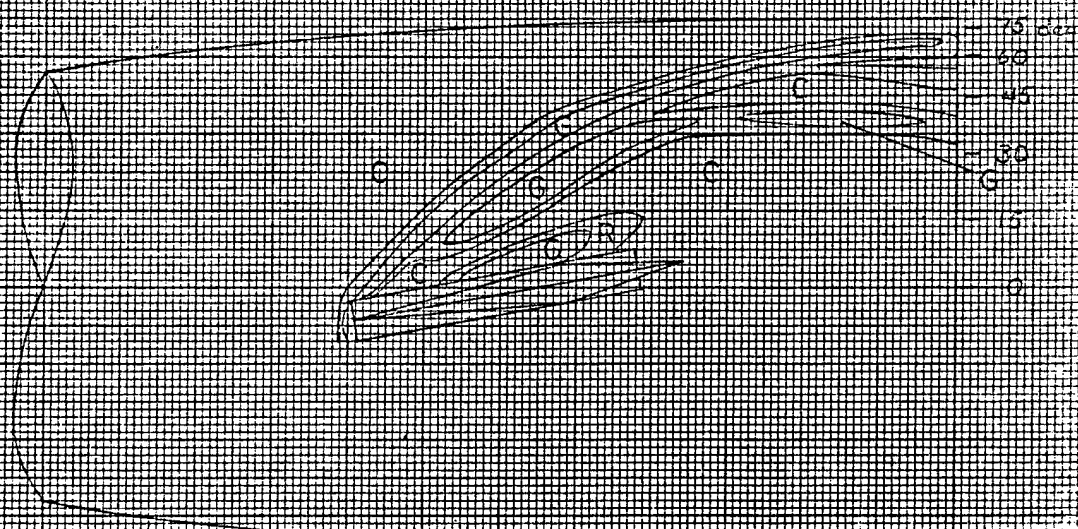
49

c. Fin 3, δr=-10 deg
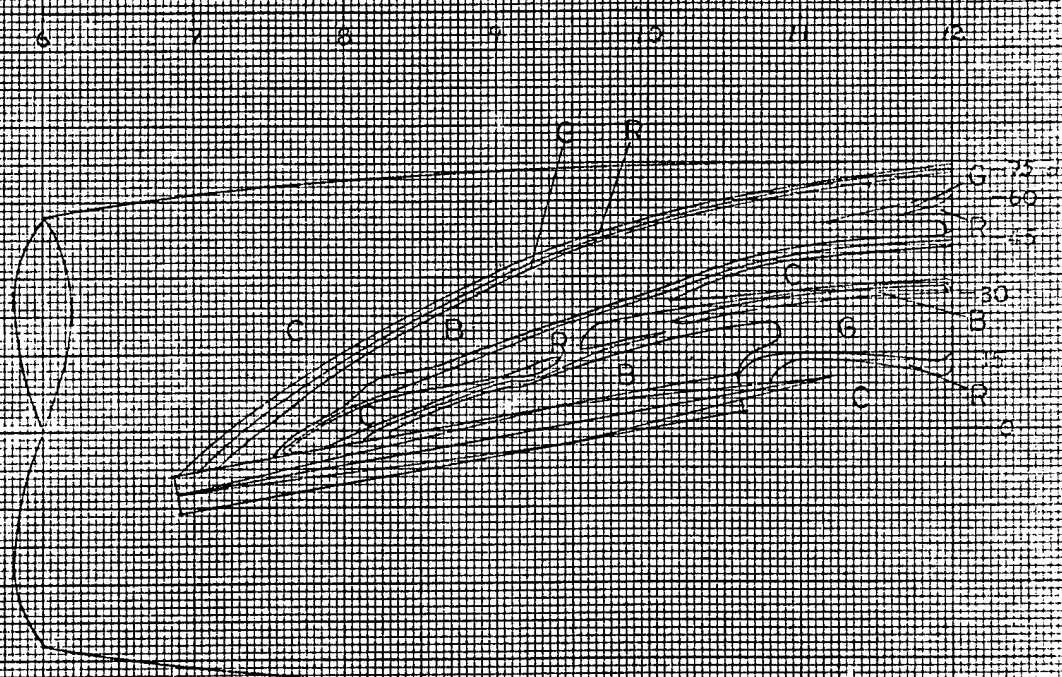
d. Fin 3, δr=-15 deg

Figure 6. (Concluded)

a. Fin A, δ=0 deg

b. Fin A, δ=10 deg

Figure 18. Temperature Profiles on Model D,
$M_\infty=30$, $Re_\infty=3.0\times10^6$/ft., $\alpha=0$ deg.

61

a. Fin A, δ=0 deg.
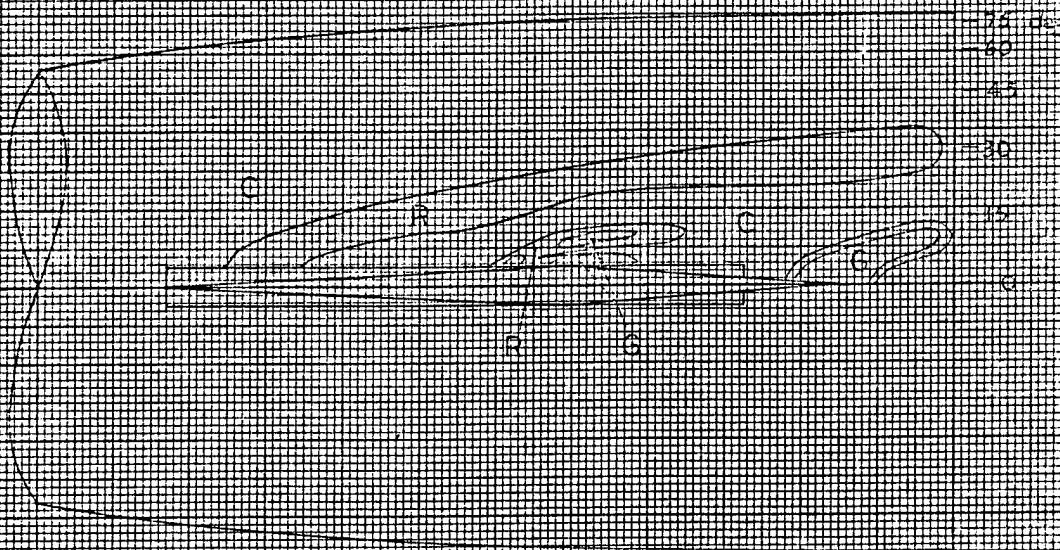
b. Fin A, δ=-10 deg.

Figure 19. Temperature Profiles on Model D,
M∞=3.0, Re∞=3.0×10⁶ft., α=5 deg.

62